

MODIFYING AN INVERTED LABORATORY MICROSCOPE FOR RAMAN
MICROSCOPY

A Thesis

Presented in Partial Fulfillment of the Requirements for
the Degree Master of Science
in the Graduate School of The Ohio State University

By

Nathan S. Gaubert

The Ohio State University
2006

Master's Examination Committee:
Professor Heather C. Allen, Advisor
Professor Richard L. McCreery

Approved by

Advisor
Graduate Program in Chemistry

ABSTRACT

It is demonstrated herein that with specific modifications a spectroscopic imaging instrument, a Raman microscope, can be constructed from a common inverted laboratory microscope and standard laser optics. All of the steps taken to build this instrument are outlined in this work, as well as all of the computer programs written to aide in spectral image reconstruction. This instrument shows the ability to perform all of the necessary duties required for a spectroscopic imaging device, specifically the ability to localize a microscopic area and collect a Raman spectrum from that area to provide image contrast.

Several different model systems were imaged with the Raman microscope to demonstrate the ability of the instrument to reconstruct the images of the samples from spectral data. All of the experiments conducted in this thesis demonstrate that the Raman microscope can accurately recreate the image of the sample being analyzed regardless of size, morphology, or chemical composition. The results of these experiments also show that the computer programs written to aide in image reconstruction can accurately take the acquired spectral data and combine it with the position data to visualize the sample in a chemically informative manner.

To
My Loving Wife and Daughter
Meredith and Marin

ACKNOWLEDGMENTS

There are many people who have been instrumental in me achieving this goal. To list them all would be impossible, but there are a few that deserve a special thank you. First of all, I would like to thank my advisor, Heather Allen, for providing the guidance and support necessary to complete the research for this degree. I would also like to thank all of the members of the Allen lab, both past and present. In particular: Dr. Laura Voss, Dr. Gang Ma, Lisa Van Loon, and Kandice Harper who were always readily available to assist when obstacles presented themselves. The discussions and brainstorming with you all was instrumental in the success of this work. You are all my dear friends. I also need to thank Dr. Terry Gustafson, even though you were not my advisor, you always had time for me to bounce ideas off of you.

A very special thank you goes to my parents. Without their constant encouragement and support, this achievement would not have been possible. You instilled in me a thirst for knowledge that is still not quenched. Last but not least I would like to thank the two most important women in my life, my beautiful wife Meredith and adorable daughter Marin. Meredith you were what kept me going when the tasks seemed too daunting and you always knew how to put a smile on my face. Marin you were my motivation and inspiration throughout all of the long nights spent in the lab finishing this project.

VITA

July 16, 1981.....Born – Rockdale, TX

2002 – 2003.....Undergraduate Research Assistant
Texas A&M University

2003.....Undergraduate Teaching Assistant
Texas A&M University

December 20, 2003.....B.S. Chemistry
Texas A&M University

2004 – 2006.....Graduate Teaching and Research Assistant
The Ohio State University

FIELDS OF STUDY

Major Field: Chemistry

TABLE OF CONTENTS

	<u>Page</u>
Abstract.....	ii
Dedication.....	iii
Acknowledgments.....	iv
Vita.....	v
List of Tables	viii
List of Figures.....	ix
Chapters:	
1. Introduction.....	1
2. Background Theory of Raman Spectroscopy and its Applicability to Microspectroscopic Imaging.....	6
2.1 – Introduction.....	6
2.2 – The Raman Effect	6
2.3 – Theory: Application of the Raman Effect to Microscopy	11
2.4 – Theory: Coherent anti-Stokes Raman Scattering (CARS).....	13
3. Experimental Set-Up and Procedures	20
3.1 – Introduction.....	20
3.2 – Raman Microscope Set-up.....	21
3.2.1 – Laser Excitation Sources.....	22
3.2.2 – The Microscope	24

3.2.3 – The Detector.....	27
3.2.4 – Spectral Acquisition Control and Post Acquisition Data Processing	29
3.3 – Raman Microscope Alignment and Calibration Procedures.....	30
3.4 – Point Illumination Imaging Procedure.....	35
4. Results and Conclusions	55
4.1 – Introduction.....	55
4.2 – Imaging Macroscopic Crystalline Naphthalene.....	55
4.4 – Imaging Microscopic Homogeneous d ₆₂ -DPPC Vesicles.....	60
4.6 – Summary of Conclusions.....	66
List of References	80
Appendices:	
Appendix A: Raman Microscope Stage Coordination using LabVIEW 7.1	83
A.1: LabVIEW Serial Port Communication Interface Modification.....	83
A.2: Operation of the Raman Microscope Coordinate Control Interface.....	85
A.3: Preparation of Microscope Position Data for use in Image Generation.	87
Appendix B: Raman Microspectroscopic Image Generation using Igor Pro 4.0	92
B.1: Procedure – Using Igor Pro for Raman Microspectroscopic Data.....	92
B.2: Image Creation using Igor Pro	98
B.2.1: Creating a Matrix of Z Values for use in Igor Pro.	98
B.2.2: Creating Contour, Image and Surface plots in Igor Pro.....	100

LIST OF TABLES

	<u>Page</u>
Table 3.1: The pin configuration for the RS-232 cable connection used to connect the digital readout to the computer.	54
Table A.1: User defined variables for Raman Microscope Coordinate control in LabVIEW.....	91
Table B.1: An example of a Z-Matrix used to aide in image reconstruction.....	106

LIST OF FIGURES

	<u>Page</u>
Figure 2.1: The Jablonksi energy diagram for Rayleigh, Stokes and anti-Stokes Raman scattering.	16
Figure 2.2: Example spectrum displaying the Rayleigh, Stokes, and anti-Stokes Raman lines. ²	17
Figure 2.3: Example of a raster scan pattern – (A) Spatially resolved points of spectral acquisition. (B) Motion of microscope stage to position sample for spectral acquisition.	18
Figure 2.4: Jablonksi energy diagram for Coherent anti-Stokes Raman Scattering (CARS).	19
Figure 3.1: Schematic of the Raman microscope set-up.....	37
Figure 3.2: Photograph of the Raman microscope set-up.....	38
Figure 3.3: Diagram of the laser excitation source and coupling optics used with the Raman Microscope.	39
Figure 3.4: The microscope used in the experimental setup and the direction of the signal and excitation beams.	40
Figure 3.5: Schematic of the longpass dichroic mirrors used in the experimental setup.	41
Figure 3.6: 820 nm DRLP transmission curve for the dichroic mirror used with 785 nm excitation light.	42
Figure 3.7: The 545 nm DRLP transmission curve for the dichroic mirror used with the 532 nm excitation light.	43
Figure 3.8: The 830 nm red Schott glass interference filter transmission curve.	44
Figure 3.9: The 800 nm longpass filter transmission curve.....	45

Figure 3.10: Transmission curve of the 550 nm longpass filter.	46
Figure 3.11: Transmission curve for the 600 nm orange Schott glass interference filter.	47
Figure 3.12: Combined filter transmission curve when using 532 nm excitation.	48
Figure 3.13: The schematic for the signal collection and detection optics used in the experimental setup.	49
Figure 3.14: The grating efficiency curves for the diffraction gratings used in the monochromator.	50
Figure 3.15: The Andor EMCCD efficiency curve.	51
Figure 3.16: A) Reference Raman spectrum of naphthalene. ^{27, 40} B) Raman spectrum of naphthalene obtained in this study.	52
Figure 3.17: Raman spectrum of naphthalene acquired using the Raman microscope and a 1200 groove/mm grating and a 20 second exposure time.	53
Figure 4.1: Spectra of a) microscope coverslip (background), b) raw naphthalene, and c) the background subtracted spectrum of naphthalene.	68
Figure 4.2: a) Contour plot of crystalline naphthalene on a coverslip. b) 3-D plot of the out-of-plane deformation intensity distribution of naphthalene on a coverslip. c) False color image of naphthalene on a coverslip.	69
Figure 4.3: Selected Raman spectra taken at different points of the coverslip showing a) (1.75, 0.75) high intensity, b) (1.0, 0.5) moderate intensity, and c) (3.0, 0.5) no intensity.	70
Figure 4.4: a) Bulk Raman spectrum of d ₆₂ -DPPC using the RamanProbe™ fiber optic system. b) Micro-Raman spectrum of d ₆₂ -DPPC obtained using the Raman microscope.	71
Figure 4.5: a) Contour plot of a d ₆₂ -DPPC crystal on the surface of a coverslip. b) 3-D plot of the CH ₂ -SS (2105 cm ⁻¹) intensity distribution of a d ₆₂ -DPPC crystal on the surface of a coverslip. c) False color image of the d ₆₂ -DPPC crystal based on the presence of the CH ₂ -SS (at 2105 cm ⁻¹).	72

Figure 4.6: a) Contour plot of d_{62} -DPPC vesicles on the surface of a coverslip, b) 3-D plot of the CH_2 -SS intensity distribution of the d_{62} -DPPC vesicles on a coverslip, and c) False color image of d_{62} -DPPC vesicles based on the presence of the CH_2 -SS.	73
Figure 4.7: Spectra of a coverslip containing d_{62} -DPPC vesicles in a) a region showing no Raman band intensity, and b) a region of high Raman band Intensity.	74
Figure 4.8: Raman spectrum of the bulk microscope coverslip covered with microscopic crystals of naphthalene and palmitic acid.	75
Figure 4.9: Contour plots of a microscope coverslip imaged base on a) the C-H stretch of naphthalene (3056 cm^{-1}), b) the CH_2 -AS of palmitic Acid (2880 cm^{-1}), and c) the combined Contour plot showing naphthalene in white and palmitic acid in black.	76
Figure 4.10: Selected spectra taken along the red ($Y=8$) line of the contour plot of naphthalene and palmitic Acid. The position of each spectrum is noted in the upper left corner of the spectrum. The peak at 3056 cm^{-1} indicates the presence of naphthalene and the peak at 2880 cm^{-1} indicates the presence of palmitic acid.	77
Figure 4.11: Three-Dimensional intensity distribution of naphthalene and palmitic acid crystals on microscope coverslip based on a) CH_2 -AS of palmitic acid, b) C-H stretch of naphthalene, and c) the combined intensity distribution of both types of crystals.	78
Figure 4.12: Microspectroscopic false color image of a microscope coverslip based on the C-H stretch of naphthalene (in white) and the CH_2 -AS of palmitic acid (in black). Zero spectral intensity is represented by the color gray.	79
Figure A.1: Raman Microscope Coordinate Control LabVIEW Block Diagram.	89
Figure A.2: Raman Microscope Coordinate Control LabVIEW Front Panel.	90

CHAPTER 1

INTRODUCTION

Raman spectroscopy allows for the characterization and identification of materials based on intrinsic molecular vibrations that are singularly unique to a specific type of molecular component of that material. Optical microscopy is used in many areas of scientific research to observe and monitor microscopic sized specimens that are not observable with the unaided human eye. The combination of an optical microscope with Raman spectroscopy, to perform micro-Raman spectroscopy, allows for the acquisition of spectroscopic data from significantly less sample than is normally required for traditional Raman spectroscopy. Micro-Raman spectroscopic techniques have been applied to the fields of materials science, environmental analysis, biology, and medicine.¹

Raman spectroscopy is used throughout the field of materials science for the identification of contaminants and defects in newly synthesized materials, as well as for the characterization of the materials themselves. Contamination and defects formed during the commercial production of many materials is a constant problem in industry, and as such, Raman spectroscopy has been used to evaluate and identify them. In many cases though, the signal from these contaminants or defects are much too small to be distinguishable from the bulk material signal. In these situations, a technique is needed to

localize a much smaller area for analysis. Micro-Raman spectroscopic techniques are ideally suited to localize a small area. For example, in semiconductor production because circuit-board geometries and their components are now consistently on the micrometer dimensions, contaminants on this size scale often produce reliability problems. Micro-Raman spectroscopy is often the only means by which these contaminants can be identified.²

In the area of environmental analysis micro-Raman spectroscopic techniques have been utilized for the identification of airborne particles that have been collected with the help of impactors.³ These airborne particles often range in size from 1 – 10 μm , which is ideally suited for micro-Raman spectroscopic studies. The investigation into these types of particles is important to many areas of human concern such as pollution monitoring and global climate change.⁴ In fact, *in situ* micro-Raman techniques have recently been employed to investigate the oxidation and possible byproducts of volatile organic compounds (VOC) when reacted with ozone.^{5,6}

Another important area of research where micro-Raman techniques are being utilized is in the fields of biology and medicine where the desire to analyze specimens at a cellular level is obvious. Micro-Raman techniques have been used to selectively analyze the components of cellular membranes as well as to study pigments in vegetable and animal single cells.⁷ Raman microscopic determination of the distribution of anti-tumor drugs within the nucleus and cytoplasm of a single living cancer cell has been shown as a possible approach to studying cancer drug effectiveness at a cellular level.⁸ Raman microspectroscopic studies are now also delving into the examination of

molecular changes in whole bone as it is stressed to study the fundamental origins of the mechanical properties of human bone.^{9, 10}

Whenever the question comes down to “what chemical species are in my sample, how much of each is present and – most importantly – where are they located?” spectral imaging is the solution. The combination of an optical microscope with the molecular specificity of Raman spectroscopy allows for even more information to be garnered than simply localizing a microscopic area for spectral acquisition as in micro-Raman spectroscopy. The combination of these two provides for the direct visualization of the spatial arrangement of a specimen based on chemical composition. The ability of Raman spectroscopy to discriminate spectrally between different components of a sample, based on their unique molecular vibrational signatures, is further enhanced by the ability of an optical microscope to append spatially resolved coordinates to this acquired molecular signature. The combination of these two instruments into a Raman Microscope provides an analytical tool that has the capability of spectroscopically imaging microscopic sized specimens. The resulting images produced by this instrument provide a distribution map of the components within a given sample area of a specimen.

Raman microspectroscopic imaging techniques are utilized in many of the same area as previously discussed with the significant difference being that this is an imaging technique compared with Raman spectroscopy being only a sampling technique. In the field of materials science, Raman microspectroscopic imaging is being utilized as a way to monitor silicon stress during the fabrication of microelectronics which can often arise from lattice mismatch among different materials, sharp patterning, and different thermal expansion coefficients. It was also shown that monitoring microelectronic devices in this

fashion allowed for the stress evaluation to continue occurring even after transparent or semi-transparent films were deposited on the original silicon substrate, due to the inherent chemical specificity of the technique.^{11,12} In biological and medical research, Raman microspectroscopic imaging has been utilized to provide additional chemically specific information to microscopic images where the added detail can differentiate between the species being studied. Raman microspectroscopic imaging has recently been employed to investigate several types of cancer including ovarian, skin, and breast cancer. Recent advances in imaging breast tissue with Raman imaging has shown the ability to possibly provide for a less invasive *in vivo* diagnosis of breast cancer.¹³

Raman imaging also provides a means to investigate functional red blood cells to monitor and understand chemical processes in the living cell. These techniques have been used to provide insight into heme aggregation and denaturation, as well as to provide information about the electronic structure of the malarial pigment haemozoin.¹⁴ Spectral imaging based on Raman microspectroscopic techniques are being developed as a tool to characterize bone microstructure. The current interest in this type of tool is in mapping the chemical species within mature and immature bone to correlate Raman signatures to known chemical properties of bone in diseases like osteoporosis as well as genetically induced diseases such as craniosynostosis and osteogenesis imperfecta.^{15, 16}

Other spectroscopic techniques are often combined with optical microscopes to image sample based on similar molecular vibrational spectral signatures. Some of the other spectroscopic techniques used for spectral imaging are second harmonic generation (SHG)¹⁷, Fourier transform Infrared absorption (FTIR)¹⁸, surface enhanced Raman scattering (SERS)¹⁹, and coherent anti-Stokes Raman scattering (CARS)²⁰. Spectral

imaging based on the CARS phenomenon especially has seen increased use as a means of studying biologically relevant samples due to its higher level of chemical sensitivity. CARS microscopy has been used for selective imaging of lipid droplets in unstained living cells with a very high level of contrast.²¹ In a recent study, CARS microscopy was applied to monitor the growth of triglyceride droplets during the differentiation process of 3T3-L1 cells.²² In addition to the traditional picture of lipid accumulation in the differentiation process, the images indicate an intermediate stage that is signified by the removal of cytoplasmic lipid droplets after addition of the induction medium. This reduction of lipid droplets was attributed to an increased activity of hormone sensitive lipase, the enzyme responsible for hydrolyzing intracellular triglyceride and sterol esters.

The intent of this thesis work is to demonstrate that a Raman microscope can be constructed from a common inverted research microscope using standard laser optics. This thesis will detail the instrument construction and calibration. This work will also discuss the procedures used to perform Raman microspectroscopic imaging, and the computer programs created to aide in image reconstruction. This work will show that the Raman microscope can image samples of varied morphology and composition spectrally. The Raman microscope will also be shown to be a viable option to characterize and visualize the composition of heterogeneous samples. Steps to further enhance and improve the current instrument will be outlined. The steps needed to convert the Raman microscope into a more spectroscopically powerful instrument, a Coherent anti-Stokes Raman (CARS) microscope, for use in future research endeavors will also be discussed.

CHAPTER 2

BACKGROUND THEORY OF RAMAN SPECTROSCOPY AND ITS APPLICABILITY TO MICROSPECTROSCOPIC IMAGING

2.1 – Introduction

Spectroscopy is an analytical technique devoted to the identification of elements and the elucidation of atomic and molecular structure by measurement of the radiant energy either absorbed or emitted by a substance.²³ One analytical technique often employed to characterize a compound using visible light is Raman spectroscopy. Raman spectroscopy has the ability to characterize a compound based on intrinsic molecular vibrations. Raman spectroscopy differs from other optical spectroscopies in that it gains information by analyzing the inelastic scattered radiation collected from a sample. The phenomenon is named after the Indian physicist, Sir Chandrasekhar Venkata Raman, who first observed the Raman Effect in 1928. Shortly after this discovery, Sir Raman was awarded the 1930 Nobel Prize in Physics. This chapter will encompass a brief discussion of the scientific principles used throughout this work.

2.2 – The Raman Effect

When a beam of monochromatic light impinges on a sample or molecule, almost all of the photons of light emerging from the sample are unchanged in either wavelength

or energy. This type of light interaction is known as either elastic scattering or more commonly Rayleigh scattering, named after Lord Rayleigh. Lord Rayleigh first described this scattering process when explaining why the sky is seen as the color blue when light from the sun strikes molecules in the earth's atmosphere. The reason for describing the nature of this type of scattering as elastic is due to the fact that, as an elastic material will return to its original form unchanged after being stretched, so will the photons of light that are scattered in this way.

While the vast majority of light bombarding a molecule will interact in an elastic fashion, a very small amount, about 1 in 10^7 molecules, will scatter photons at different wavelengths and energies from the incoming photons.²³ The differences in wavelength and energy are due to inelastic scattering processes. This type of scattering is indicative of a molecular vibrational mode being excited. When this type of event occurs, the scattered photons will be lower in energy, and thus longer in wavelength than the incoming radiation. Light can also scatter off of a vibrationally excited molecule, in which case the scattered photons will be higher in energy than the incoming light. Analysis of these changes in wavelength from the incident wavelength yield molecular information about the sample being analyzed. This inelastic scattering of light is what is known today as the Raman Effect. A Jablonski diagram illustrating both Rayleigh scattering and the Raman Effect is shown in Figure 2.1.

After interacting with a molecule, the scattered photons of light can either be of higher or lower energy than the incident photons, as previously mentioned. This difference in frequency ($\Delta\nu$), between what is known as the Raman line and the Rayleigh line will correspond to fundamental vibrational frequencies that are intrinsic to the

scattering molecule. It is important to note that molecular vibrations can be of several different types including stretching, bending, torsion, and deformation. Although stretching molecular vibrations will produce stronger peaks than bending molecular vibrations, bending molecular vibrations are very useful in differentiating similar types of bonds. It is the correspondence between molecular vibrational frequency and the shift in incident light frequency that allows Raman spectroscopy the ability to gain specific molecular level insight of a sample.

Raman lines are divided into two regimes depending on whether the scattered photons are higher or lower in energy compared to the incident photons of light. When the energy of the scattered photon is less than the energy of the incident photons ($\nu - \Delta\nu$) what is known as a Stokes transition occurs. A Stokes transition gives rise to a Stokes line in the Raman spectrum. When the energy of the scattered photons is more than the energy of the incident photons ($\nu + \Delta\nu$) an anti-Stokes transition occurs. This gives rise to what is known as an anti-Stokes line in the Raman spectrum. Both the Stokes and anti-Stokes lines are symmetric about the Rayleigh line because they both correspond to the same vibrational quanta of energy ($\Delta\nu$) that is either gained or lost by the incident photons of light (Figure 2.2).

The Stokes lines are much more intense than the anti-Stokes lines at room temperature owing to the fact that anti-Stokes transitions can only occur from an excited vibrational state which is less probable to occur than a transition originating from the molecular ground state.² The designation of which set of Raman lines would be named Stokes and anti-Stokes originated from Stokes' Law which states that the frequency of fluorescent light is always less than or at most equal to the frequency of the exciting light.

The lines in the Raman spectrum that “obeyed” Stokes’ law were named Stokes lines and ones that “disobeyed” Stokes’ law were named anti-Stokes lines even though there are many differences between the Raman Effect and fluorescence.²⁴

For the Raman Effect to be observable there must be electric dipole radiation emitted from a molecule. Remember that the Raman Effect is based on inelastic scattering, and that scattering in general, occurs because an electric field can induce a dipole in a molecule. Another way of stating this is that the polarizability of the molecule must change with the motion (vibrational or rotational) of the molecule. The polarizability of a molecule can be expressed as in Equation 2-1,

$$\vec{P} = \alpha \cdot \vec{E} + \left(\frac{1}{2}\right)\beta \cdot \vec{E} \cdot \vec{E} + \left(\frac{1}{6}\right)\gamma \cdot \vec{E} \cdot \vec{E} \cdot \vec{E} + \dots \quad (2-1)$$

where α , β , and γ are tensors. A tensor is an array of numbers, or functions, that transform according to certain rules under a change of coordinates.²⁵ The polarizability is an induced electric dipole moment. The polarizability is typically approximated by the first polarizability tensor, α . The work in this thesis will continue to use this first order approximation of the polarizability function. Equation 2-1 can then be rewritten as Equation 2-2,

$$\vec{P} = \alpha \cdot \vec{E} \quad (2-2)$$

where all of the higher order terms have been left out of the polarizability equation.

When the electric field vector (\vec{E}) is assumed to be sinusoidal in nature

$$\vec{E} = \vec{E}_0 \cos(2\pi\nu_0 t) \quad (2-3)$$

then equation 2-2 can be rewritten as

$$\vec{P} = \alpha \cdot \vec{E}_0 \cos(2\pi\nu_0 t) \quad (2-4)$$

A Taylor expansion can be performed on the polarizability tensor α ,

$$\alpha = \alpha_0 + \left(\frac{\partial \alpha}{\partial Q_k} \right)_0 Q_k + \dots \quad (2-5)$$

which approximates the total polarizability along a given normal coordinate, Q_k .

Remembering that we have assumed a sinusoidal wave for the electric field vector then

Q_k becomes

$$Q_k = A_k \cos(2\pi\nu t) \quad (2-6)$$

When equation 2-6 is substituted back into equation 2-5, the polarizability tensor becomes

$$\alpha = \alpha_0 + \left(\frac{\partial \alpha}{\partial Q_k} \right)_0 A_k \cos(2\pi\nu t) \quad (2-7)$$

Equation 2-7 can then be substituted into equation 2-4 to yield a fully expanded expression of the polarizability equation which is rewritten as Equation 2-8.

$$\vec{P} = \alpha_0 \cdot \vec{E}_0 \cdot \cos(2\pi\nu_0 t) + A_k \cdot \vec{E}_0 \cdot \left(\frac{\partial \alpha}{\partial Q_k} \right)_0 \cdot \cos(2\pi\nu_0 t) \cdot \cos(2\pi\nu t) \quad (2-8)$$

If the identity for the product of two cosines, $\cos \alpha \cdot \cos \beta = \frac{1}{2} \cos(\alpha - \beta) + \frac{1}{2} \cos(\alpha + \beta)$

is used, then Equation 2-8 becomes

$$\vec{P} = \alpha_0 \vec{E}_0 \cos(2\pi\nu_0 t) + \frac{1}{2} \left(\frac{\partial \alpha}{\partial Q_k} \right)_0 A_k \vec{E}_0 \cdot [\cos(2\pi\{\nu_0 - \nu\}t) + \cos(2\pi\{\nu_0 + \nu\}t)] \quad (2-9)$$

The first term of Equation 2-9 corresponds to the unshifted scattered light or Rayleigh scattered light. The second term gives rise to two new frequencies those at

$\nu_0 - \nu$ and $\nu_0 + \nu$. These new frequencies are the Stokes ($\nu_0 - \nu$) and the anti-Stokes ($\nu_0 + \nu$) frequencies. The selection rule for Raman spectroscopy is expressed mathematically as

$$\left(\frac{\partial \alpha}{\partial Q_k} \right)_0 \neq 0 \quad \text{(2-10)}$$

This selection rule implies that for a Raman transition to occur at least one component of the polarizability tensor along a given coordinate must be non-zero.^{24, 26-28}

2.3 – Theory: Application of the Raman Effect to Microscopy

For many years Raman spectroscopists have collected spectral data, either from a large amount of sample material or from a specific region of the sample. This technique yields information about the local composition of the sample, but does not provide an overview of the spatial arrangement of the various molecular species within a heterogeneous sample.²⁸ By coupling a monochromatic light source into a microscope equipped with a Raman spectrometer, a powerful analytical tool is created that allows for the direct mapping of the spatial arrangement of an inhomogeneous sample. To map the spatial arrangement of a heterogeneous sample, the Raman spectrum is monitored as a function of position in the sample. Chemical discrimination between sample components is dependent on spectral differences between the various components. Spatial discrimination is dictated by the movement of the microscope stage and the focused spot diameter.

A Raman microspectrometer works in much the same fashion as a traditional Raman spectrometer. A beam of monochromatic radiation strikes a sample and the scattered is then collected and passed through a dispersive monochromator before

striking a detector for spectral data collection. One of the differences between a traditional Raman spectrometer and the Raman microspectrometer used in this work, other than the obvious difference in sample size, is that the Raman microspectrometer employs 180° , or backscatter, detection geometry, rather than the more conventional 90° detection geometry.^{27,28} In traditional Raman spectroscopy, the scattered light is detected at an angle of 90° relative to the incident light to reduce the elastic scatter entering the spectrometer so as to not overwhelm the Raman spectrum. In the Raman microspectrometer used in this work, the microscope objective used to deliver and focus the incident light onto the sample is also used to collect any 180° backscattered light from the sample and then direct it to the detector. Band rejection filters are necessary to adequately filter out the incident light before detection in this set-up. However, this 180° detection geometry allows for easy detection from a single position without the hassle of coordinating the motion of multiple microscope objectives to deliver the incident light and to collect the signal.

There are several techniques used to create an image of a sample based on its intrinsic Raman vibrational spectrum. Several techniques that have been employed by others in the past include direct or global imaging,²⁹ line illumination,^{27,30} and point illumination.³¹ The last two techniques are known as series-imaging techniques because they require image reconstruction of the sequential spectra taken of the sample. These are obtained by scanning the sample either point by point or line by line as dictated by the experimental set-up. The imaging technique used in this work is point illumination where the sample on the microscope stage is moved sequentially in a raster pattern over the laser spot generated by the microscope objective. At each resolved position of the

sample a signal is collected by the same microscope objective providing the incident light. The signal is then directed towards a dispersive monochromator and then detected by a charged coupled device (CCD) detector. An example of a raster pattern used when scanning a sample in this method is illustrated in Figure 2.3.

Point illumination Raman imaging is very time consuming because a spectrum must be collected at each point along the sample surface. The use of a multichannel detector such as the CCD detector allows for the collection of an entire Raman spectrum at each point in a minimal amount of time. Once the entire sample area is scanned, an image recreation routine like the one outlined in Appendix B must be employed to recreate the image of the sample. This means that the image is not readily available to view until after all spectra have been collected and the data has been properly worked up. The images created in this fashion garner their contrast by the presence or absence of a molecular vibration.

2.4 – Theory: Coherent anti-Stokes Raman Scattering (CARS)

Since the first introduction of the Raman microscope in 1973, optical and laser technology has made tremendous advances.³² The availability of inexpensive, energy-efficient, stable, and reliable laser sources, together with the improved technology for spectral filtering and multi-channel detection has greatly increased the ease of study of inorganic and organic materials. Despite the obvious advantages of being a very informative and almost non-destructive method of studying biological molecules, spontaneous Raman spectroscopy suffers from a series of limitations such as a fluorescent background and a low signal level. Non-linear Raman spectroscopy and, in particular, spectroscopy based on coherent anti-Stokes Raman scattering (CARS), can

resolve most of the problems associated with conventional spontaneous Raman spectroscopy.³³

The first systematic study of the nonlinear Raman process, which would later become known as coherent anti-Stokes Raman scattering, was carried out by P. D. Maker and R. W. Terhune at the Ford Motor Company in 1965, as a way of studying combustion reactions with organic liquids.³⁴ The name coherent anti-Stokes Raman scattering (CARS) spectroscopy did not actually appear in literature until nine years later, in 1974.³⁵ CARS is a third-order nonlinear four-wave mixing optical process involving a pump and a Stokes probe laser beam at frequencies of ω_p and ω_s . When these two beams are focused into a sample at sufficient power, a third beam of frequency ω_{as} , is generated as in Equation 2-11.

$$\omega_{as} = 2 \cdot \omega_p - \omega_s \quad (2-11)$$

The intensity of the signal generated at this ω_{as} is normally very weak until the frequency difference $\omega_p - \omega_s$ coincides with the frequency of a Raman-active molecular vibration of a sample (Ω).³⁶ At this frequency the CARS signal is strongly enhanced and is actually much more intense than the spontaneous Raman signal of the same molecular vibration.³⁷ The Jablonski energy diagram of CARS can be seen in Figure 2.4.

As CARS is a four-wave mixing process, the signal intensity depends nonlinearly on the incident intensities

$$I_{CARS} \approx I_p^2 \cdot I_s \quad (2-12)$$

where I_p is the intensity of the pump beam and I_s is the intensity of the Stokes probe beam. Since the intensity of these pulses is greatest in the focal point of the microscope,

CARS spectroscopy offers excellent discrimination against out-of-focus signal collection. A CARS microscope is an ideal confocal microscope without using an additional aperture for confocality,³⁸ thus greatly increasing the signal collection efficiency. Similar to other nonlinear optical processes, high peak powers are necessary for the efficient generation of a CARS signal. These are readily available using femtosecond or picosecond light pulses, the choice of which is determined by the spectral resolution required for the system being studied.

The application of the CARS process to microscopy has developed into an important method for chemical imaging. In CARS microscopy, the temporally and spatially overlapped pump and Stokes laser pulses are tightly focused into a sample to generate a signal in a small excitation volume ($< 1 \mu\text{m}^3$).³⁹ With the tight focus that using a high numerical aperture lens provides, the phase-matching conditions are relaxed because of the large cone of wave vectors and the short interaction length.²⁰ The CARS image is acquired by raster scanning the sample or the laser beams, much like spontaneous Raman microspectroscopic imaging is done. CARS images can be acquired by the same techniques as those used for spontaneous Raman microscopy images. Because the CARS intensity has a quadratic dependence on the pump field intensity and a linear dependence on the Stokes field intensity, the signal is generated from a small volume in the central focal region. This provides CARS microscopy with a high 3D sectioning capability that is much superior to spontaneous Raman microscopy.³⁷

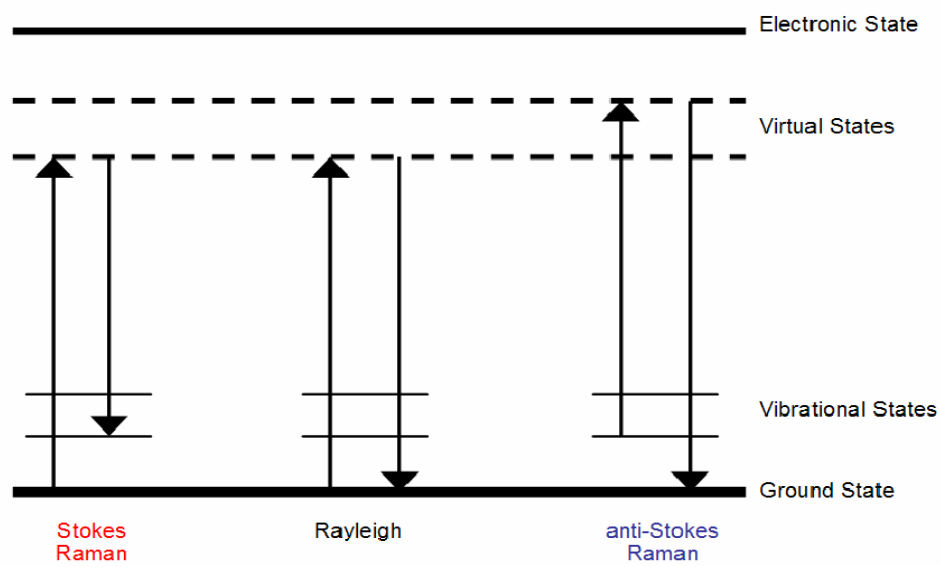


Figure 2.1: The Jablonski energy diagram for Rayleigh, Stokes and anti-Stokes Raman scattering.

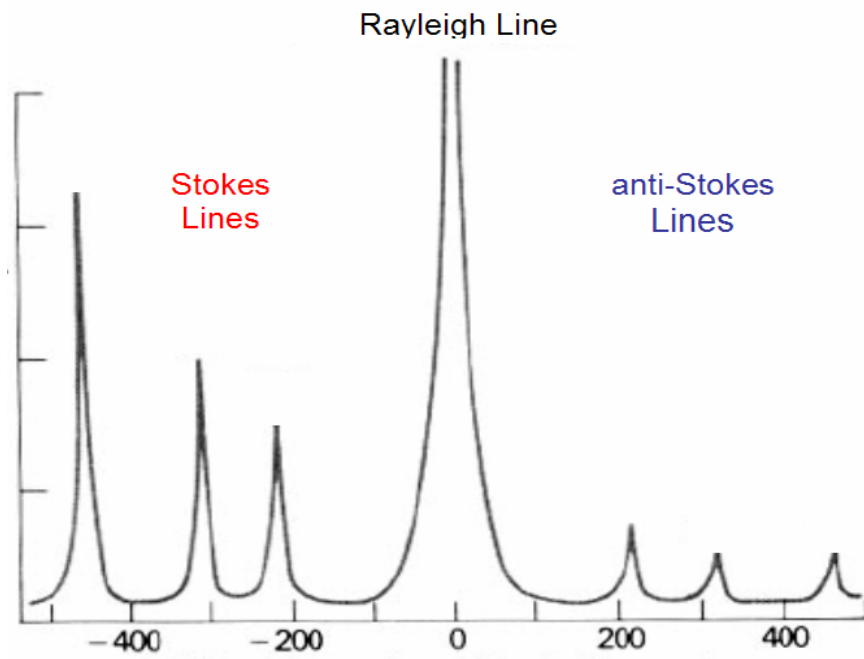


Figure 2.2: Example spectrum displaying the Rayleigh, Stokes, and anti-Stokes Raman lines.²

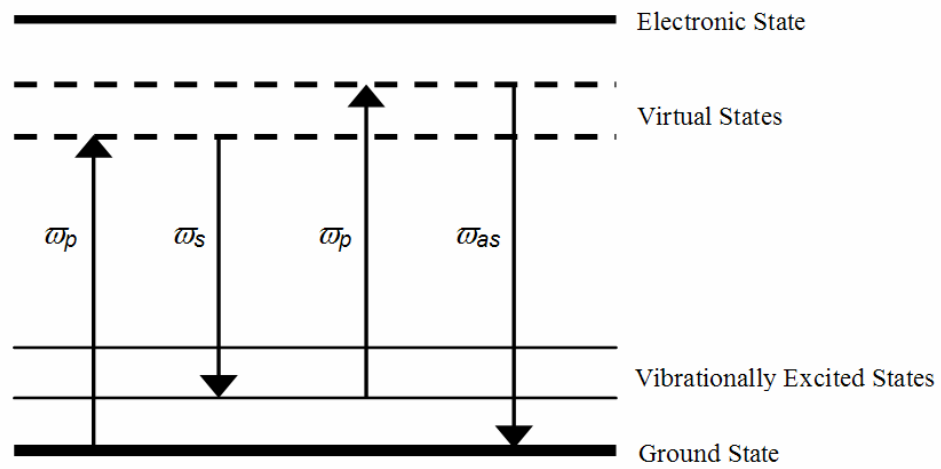


Figure 2.4: Jablonski energy diagram for Coherent anti-Stokes Raman Scattering (CARS).

CHAPTER 3

EXPERIMENTAL SET-UP AND PROCEDURES

3.1 – Introduction

The original intent in building a spontaneous Raman microscope was as a stepping stone toward the creation of a coherent anti-Stokes Raman Scattering (CARS) microscope. CARS microscopy allows for much better depth resolution, and eliminates the problems of a strong fluorescent background and weak signal strength that can plague spontaneous Raman spectroscopy. The CARS signal occurs at a higher frequency than one photon fluorescence. This allows for the detection of the CARS signal even in the presence of a high fluorescent background.²⁰ The problem of one photon fluorescence in spontaneous Raman spectroscopy can sometimes be avoided by using longer wavelength excitation sources. However, the detection of the Stokes shift from longer wavelength excitation can be difficult due to the lack of efficiency of many detectors at these longer wavelengths.

CARS microscopy gets its superior depth resolution because as a nonlinear technique, the signal is only generated at the laser focus of the objective. This allows for very specific point by point three dimensional images to be obtained from thick samples, something which is impossible to do with spontaneous non-confocal spontaneous Raman

microscopy. With non-confocal spontaneous Raman microscopy all of the molecules that come into contact with the light source can contribute to the overall signal obtained. This can make it impossible to discern, with any certainty, whether or not the signal is derived specifically from the focal point or from an out of focus point.

By first building a spontaneous Raman microscope, the difficulties of combining two different excitation sources in the microscope to generate the nonlinear response in CARS microscopy can be avoided. A spontaneous Raman microscope also does not require a tunable infrared excitation source, such as an optical parametric amplifier (OPA), to create the assorted Stokes pulses needed to generate a CARS spectrum. This chapter will deal with the experimental setup for the Raman microscope, the steps needed to align and calibrate the instrument, and the procedures used to acquire the necessary data needed for spectral imaging.

3.2 – Raman Microscope Set-up

The Raman microscope set-up consists of four primary sections: a laser excitation source, a microscope, a detector, and a computer for spectral acquisition and image reconstruction. A substantial amount of effort and care was needed to combine these together to build a functioning Raman microscope capable of recreating an image of a sample based on its intrinsic molecular vibrational signature. The remainder of this section will detail each of the individual components and any additional materials needed to combine them together. The procedures used to align and calibrate the microscope, as well as the procedures used in imaging a sample are also discussed. The experimental set-up is shown in Figure 3.1, and a photograph of the completed experimental setup for the Raman Microscope is shown in Figure 3.2.

3.2.1 – Laser Excitation Sources

The Raman microscope currently has two laser excitation sources at its disposal: a visible source (532 nm) and a near-infrared (NIR) source (785 nm). The choice between excitation sources depends on the type of molecular vibration of the sample to be imaged. There are several reasons for using multiple excitation sources such as the grating and detector efficiencies, and the lack of proper filters needed to filter out excess incident light. Primarily the coating on the CCD detector has a cut off wavelength of 1000 nm, Figure 3.15. This means that wavelengths greater than 1000 nm aren't detected efficiently. In fact, the efficiency at wavelengths shorter than 1000 nm is not adequate to detect the weak Raman signal. This presents a huge problem when using the NIR excitation source at 785 nm because Raman shifts greater than $\sim 2740\text{ cm}^{-1}$ are not efficiently detected by the CCD detector used. This means that molecular vibrations that appear in the ~ 2740 to 4000 cm^{-1} region are not easily available for use as a basis for imaging. Key spectral features, such as the CH modes are very weak with 785 nm excitation to begin with, so any additional detector inefficiency creates a problem.

To circumvent this problem, a visible excitation laser source at 532 nm was employed when C-H stretching modes needed to be detected. This is not a perfect solution to the efficiency problem because the visible light source suffers from a current lack of efficient filtering of the incident light. A 532 nm notch filter could be purchased to alleviate the problem of inefficient filtering. Unfortunately the use of visible laser light can also induce fluorescence with certain molecules, such as molecules with

conjugated π -bonds. Therefore, the visible light source was used only when the NIR light source could not be employed.

Near-Infrared Excitation Source. The NIR laser excitation source used in this instrument is a 785 nm, frequency-stabilized, continuous wave (CW) diode laser from Process Instruments Inc. The output can be tuned from 150 to 250 mW. The beam is horizontally polarized when exiting the main housing of the laser, but becomes scrambled when the laser light is coupled into a fiber optically coupled Raman probe (that delivers the laser light to the experimental setup). The laser light is coupled to a RamanProbe™ (InPhotonics) via a 105 μm fiber. The RamanProbe™ coupled to the 785 nm laser is used routinely to collect bulk Raman data because it has the unique ability to deliver the excitation light, collect the Raman shifted light, and filter out the Rayleigh scattered light collected with the Raman signal.

In this experimental setup the RamanProbe™ was used as an excitation source only, not for the collection of signal. The RamanProbe™ is held in place by a custom build aluminum holder attached to a standard post mounted near the microscope. The divergent 785 nm light is roughly collimated by use of a plano-convex lens, L1 (LA1540, $d = 12.7$ mm, $f = 15$ mm, Thorlabs, Inc.). It does not need to be perfectly collimated as the microscope objectives focus the light more efficiently when the light entering the objective is slightly defocused or divergent.²⁸ The plano-convex lens is necessary to maintain the beam diameter at a minimum size, to minimize power losses from clipping any mirrors or other optics once the laser light is introduced into the microscope. After the light passes the plano-convex lens, two protected silver turning mirrors, M1 and M2 (PF10-03-P01, $D = 25.4$ mm, Thorlabs, Inc.), mounted in adjustable kinematic mirror

mounts (KM100, Thorlabs, Inc.) are used to properly align the beam into the microscope. A diagram of the laser source is shown in Figure 3.3.

Visible Excitation Source. The visible laser excitation source used in this instrument is a Millennium II diode-pumped, solid state laser from Spectra Physics. The Millennium II is a diode pumped Nd:YVO₄ solid state laser frequency doubled to operate at 532 nm. The output power of the Millennium II is tunable with a maximum output power of 2 W. The laser light emitted from the Millennium II is vertically polarized; however, the polarization is scrambled upon introduction to the 105 μm fiber of a 10 meter long RamanProbe™ (InPhotonics). The 532 nm light is focused into the fiber optic using a short focal length BK7 plano-convex lens (LA1131, $d = 25.4$ mm, $f = 50$ mm, Thorlabs, Inc.). The 532 nm laser light is by the RamanProbe™ to the microscope in the same fashion as described for the 785 nm laser excitation. The switching between excitation sources very easy since both light sources are delivered by similar RamanProbes™. This allows for the same holder to be used and only minor adjustments to the turning mirrors are needed to align the beam correctly.

3.2.2 – The Microscope

The heart of any microscopic system is the actual microscope and its objectives, which allow for collection of spectroscopic data from an extremely tiny and well defined region of the sample. The microscope used in this instrumental set-up is a Nikon TE 2000S inverted research microscope equipped with an epi-fluorescence attachment. A diagram of the microscope is shown in Figure 3.4.

The Nikon TE 2000 series microscope was chosen because its open architecture allowed for easy conversion to a Raman microscope. The epi-fluorescence attachment

allows the laser beam to be introduced easily into to the microscope objective with minor modifications. The epi-fluorescence attachment is the only open portal to the microscope. It has a mounted turning mirror and places to mount irises for alignment purposes. The epi-fluorescence attachment is modified for laser beam delivery by removing the fluorescent light source (a mercury arc lamp) and the illumination lens. With their removal, the epi-fluorescence attachment is now open for delivery. Irises were mounted inside to aid with beam alignment.

After passing through the irises inside the epi-fluorescence attachment, the light passes to the filter wheel. The filter wheel allows the user to switch between dichroic mirrors depending on which excitation source is employed. A schematic of a dichroic mirror is provided in Figure 3.5. The filter wheel can hold up to six filter holders. When using the 785 nm light for excitation, a Nikon filter holder is outfitted with an 820 nm longpass dichroic mirror (25.7 X 36 mm, 820DRLP, Omega Optical). The mirror reflects the 785 nm light and transmits wavelengths greater than 820 nm. The transmission spectrum of the 820 nm dichroic mirror is shown in Figure 3.6.

The 820 nm dichroic mirror was chosen because the transmittance of 785 nm light is less than 5%. It provides an efficient means of filtering out the incident Rayleigh light which can overwhelm parts of the Raman spectrum. When using the 532 nm light for excitation, a Nikon filter holder is outfitted with a 545 nm longpass dichroic mirror (25.7 X 36 mm, 545DRLP, Omega Optical). This mirror reflects the 532 nm light and transmits wavelengths greater than 545 nm. The 545 nm dichroic mirror was chosen because it transmits only 10% of the 532 nm light but transmits more than 50% of the

545 nm light. The transmission curve for the 545 nm longpass dichroic filter is shown in Figure 3.7.

From the dichroic mirror, the incident beam is sent to one of two microscope objectives currently in use in the Raman microscope. The first objective used is a 10X 0.60 NA objective with a 10.5 mm working distance that is initially used to locate the sample on a microscope slide. The second objective is a 100X 1.30 NA oil immersion objective with a 0.20 mm working distance used for the spectroscopic imaging of a sample. The immersion oil is type DF immersion oil, meaning it is non-fluorescent. The calculated spot size for this objective, using equation 3-1, is 3.32 μm when using 785 nm light and 2.25 μm when using 532 nm light.²⁷

$$2w_o = \frac{1.27 \cdot \lambda \cdot f}{w_\ell} \quad (3-1)$$

The objective focuses the excitation beam through the immersion oil and a coverslip to strike the sample wherever it is in contact with the coverslip. The coverslips must be #1.5 coverslips, which have an average thickness between 0.15 and 0.19 mm. This is because the working distance of the microscope objective is only slightly greater than the thickness of the coverslip supporting the sample.

The coverslips supporting the samples are placed on a micrometer controlled linearly-encoded microscope stage built by Nikon (model T-SR) equipped with a slide glass holder (model C-HSG). The microscope stage has a maximum travel distance of 75 mm in the latitudinal (or X) direction and 50 mm in the longitudinal (or Y) direction. The minimum spatial resolution of all of the images generated by the Raman microscope is governed by the minimum stage movement, which is 0.5 μm , in both the X and Y

directions. Both latitudinal and longitudinal encoders are connected to a Boeckeler Instruments Microcode II digital readout device that translates the movement of the stage into a distance measurement. Backscattered light from the sample is collected with the same microscope objective that directs the excitation light. The backscattered light is passed through a dichroic mirror and directed out the side exit port of the microscope to the detector.

3.2.3 – The Detector

The detector and the signal collection optics are diagramed in Figure 3.13. The divergent backscattered light that exits the side port of the microscope is collected and refocused by a primary BK7 biconvex focusing lens, L2 (LB1889, $d = 50.8$ mm, $f = 250$ mm, Thorlabs, Inc.). The center of the exit port of the microscope is at 3.5 inches off of the table and the entrance slit to the spectrometer is 5 inches off of the table so a periscope was built to elevate the backscattered light to the same height as the detector. The periscope consists of two protected silver mirrors, M3 and M4, mounted onto a 14 X 1.5 inch mounting post (P14, Thorlabs, Inc.) with adjustable kinematic mirror mounts (KM100, Thorlabs, Inc.) attached to 1.5 inch post clamps (C1500, Thorlabs, Inc.). The focal point of the focusing lens is situated between the two mirrors of the periscope. A protected silver turning mirror, M5 then turns the light 90° toward the detector.

Two irises along with the turning mirror and the top mirror of the periscope are used to direct the signal beam into the spectrometer. Longpass filters are placed after this turning mirror to filter out any residual excitation light. A red Schott glass interference filter or an 800 nm longpass filter is used when 785 nm light is the excitation source. The transmission curves for these filters are shown in Figures 3.8 and 3.9. A 550 nm longpass

filter and a 575 orange Schott glass interference filter are used in combination when the 532 nm light is used for excitation. The transmission curves for both of these filters are shown in Figures 3.10 and 3.11. A combined transmission curve for this filter configuration is shown in Figure 3.12. After the light passes the filters, one final lens L3 (LB1951, $d = 25.4$ mm, $f = 25$ mm, BK7, Thorlabs, Inc.) must be used to focus the light to the entrance slit of the monochromator. This ensures that the cone of light properly enters the spectrometer for detection.

The detector is an Andor Shamrock dispersive monochromator equipped with an Andor Newton electron multiplying charge coupled device (EMCCD). The Andor Shamrock is a 303 cm focal length monochromator equipped with triple grating computer controlled turret. The turret contains one each of a 300, 600, and 1200 grooves/mm grating, blazed at 500 nm. The efficiency curves for these gratings are shown in Figure 3.14, and the efficiency curve for the detector is shown in Figure 3.15. As has been mentioned previously, the cut off wavelength of the detector is around 1000 nm. From the grating efficiency curves it is also noted that the wavelengths where spontaneous Raman shifts occur, are not detected efficiently when using 785 nm light for excitation. It should be noted that the detector was chosen to be most efficient when used with a CARS microscope, where the wavelengths to be detected are in the range of 400 to 600 nm. All spectra for microspectroscopic imaging were collected using the 1200 grooves/mm grating to allow for maximum spectral peak resolution. The entrance slit width of the monochromator can be adjusted from a minimum of 10 μm to a maximum of 2,500 μm . For the experiments conducted in this work the entrance slit width was varied from 100 to 250 μm .

Raman spectra were collected with the Andor Newton EMCCD (Andor Technology DU971N-UVB, 1600 X 400 pixel array, 16 μm square pixels, back illuminated) which can be thermoelectrically cooled to $-80\text{ }^{\circ}\text{C}$ to sufficiently reduce dark current. Spectra were acquired using Andor Technology's MCD version 4.21 software. Acquisition times depended on the sample being imaged. For example, the entrance slit width when imaging naphthalene crystals was set to 100 μm and the entrance slit width when imaging d_{62} -DPPC was set to 250 μm . The CCD chip was set to full vertical binning mode (FVB) to further enhance the S/N ratio of the collected spectra.

3.2.4 – Spectral Acquisition Control and Post Acquisition Data Processing

The monochromator and its gratings, the EMCCD detector, and the recording of the microscope stage position are all controlled through a laboratory desktop computer. Some of the important minimum requirements needed to properly run both the EMCCD and the monochromator are that the computer's processor should be operating at a minimum speed of 1 GHz, and a minimum of 256 MB of RAM is needed. The computer must be equipped with at least two USB 2.0 input ports to properly transmit data to and from both the EMCCD and the monochromator. These system requirements are important when deciding which computer to use to control the detection system because if any of these three requirements are not satisfied then the detection system will not function properly and detection errors will occur. The desktop computer used in this set-up operates at a speed of 2.33 GHz, has 512 MB of memory, and has multiple USB 2.0 ports.

As has been previously mentioned, both the EMCCD and the monochromator are connected to the desktop computer via USB 2.0 cables supplied by Andor Technology.

The Boeckeler Instruments Microcode II digital readout device is connected to the desktop computer via a custom made RS-232 9 pin cable to the serial port of the computer. The cable configuration is shown in Table 3.1. The proper pin configuration was required so as to allow proper transmission of data from the digital readout device to the serial port of the computer. The monochromator and EMCCD are both controlled through Andor's MCD software version 4.21. The position of the microscope stage is monitored and recorded using LabVIEW software written expressly to communicate with the RS-232 cable connected to the computers serial port. The position of the microscope stage is captured and saved to a text file as outlined in Appendix A. All data post processing and image generation is carried out using Igor Pro. A detailed description of the macros created in Igor can be found in Appendix B.

3.3 – Raman Microscope Alignment and Calibration Procedures

Proper alignment is always a concern when dealing with optical systems, especially when dealing with a process that is inherently weak in nature. Such is the case in Raman microscopy. In this experimental setup there are two areas where the alignment is critical to the overall success of the spectral acquisition and imaging capabilities of the instrument. First, the alignment is critical for the introduction of the laser excitation source to the microscope. Second, the alignment of the backscattered signal into the monochromator must be exact. If the laser excitation source is not properly aligned upon entry into the microscope, and specifically into the microscope objective, then the light will not be properly focused onto the sample. When the collected signal is not properly aligned into the monochromator a whole host of problems can arise, the most important is the dispersed signal not falling onto the CCD chip

properly. When the signal does not strike the CCD detection chip properly, all spectral information is lost.

Proper alignment of the laser excitation source begins with securing the Raman probe of choice into the probe holder by tightening the set screw to hold it in place. Next, the focusing lens, L1, should be positioned so that the center of the laser passes through the center of the lens. The lens holder is mounted on a micrometer controlled stage that is used to adjust the lateral position of the lens. Height adjustments are made by releasing the post holder set screw and adjusting the post height. Once the laser is passing through the center of the lens and the lens face is parallel to the face of the Raman probe, the laser can be aligned into the microscope. Using two mirrors and two irises a straight laser line into the microscope objective can be assured in much the same manner as when aligning any laser line.

To start, turn the objective wheel of the microscope to a position that does not have an objective mounted in it, and remove the plug. Place a white sheet of paper on the microscope stage above the open objective mounting hole. The beam spot on this paper is used to monitor the laser alignment. Locate the two irises built into the epifluorescence attachment. The first iris will be used when turning the first mirror, M1, and the second iris will be used when turning the second mirror, M2 in Figure 3.3. (This is very similar to standard laser alignment procedures). With the unaligned laser passing through the irises and onto the paper placed on the stage, close the first iris until the opening is slightly larger than the beam diameter. Adjust M1 until the laser beam is in the center of the opening created by the first iris. Fully open the first iris. Next, repeat the same procedure using the second iris and M2. Close the second iris until the opening

is slightly larger than the beam diameter and make adjustments to M2. Continue these two steps until either iris can be closed and the beam appears in the center of the opening. When this process is done correctly the laser used for excitation will be properly aligned into the objective.

Once the excitation source is properly aligned into the microscope objective, the collected backscattered signal must be properly aligned into the monochromator. First, turn on the condenser light and choose the 100X objective. This collected white light is used for aligning the collected signal into the monochromator. The first step is to position the primary focusing lens (the 50.8 mm biconvex lens), L2, so that the lens is roughly centered about the exiting signal beam (Figure 3.13). To ensure that the lens is in the proper position, two irises are placed along the intended path that the signal beam should traverse. The center of both irises should be at a distance of 3.5 inches off of the table to match the center of the side exit port of the microscope. Adjust the tilt and position of the lens until the signal beam can pass through both irises without requiring further adjustment.

Reposition the periscope and the turning mirror so that the collected white light is directed towards the monochromator. The focal point of the primary focusing mirror, M2, should lie between the two mirrors of the periscope. To ensure that the signal is traveling straight into the monochromator, place two more irises along the intended path of the signal beam. The centers of both irises must be 5 inches above the table top. This height corresponds to the center of the entrance slit on the monochromator. To align this final leg into the monochromator close the first iris and adjust M4 until the beam of light is centered. Open the first iris and close the second one and adjust the turning mirror

until the beam of light is centered. Repeat this process until no further adjustments of either mirror is needed.

Once the beam of collected light is straight into the monochromator replace the secondary focusing lens, L3, with the curved portion of the lens facing away from the monochromator. Check the back reflection off of this lens to make sure it is buried in the path of the signal beam. Verify that the position of the focused light at the face of the entrance slit is centered going into the monochromator. Reinsert the filters before the lens and make sure the light is striking the center of the filter. The back reflection off of the filters should be parallel to the incoming beam of light.

With the excitation laser properly aligned into the microscope and the collected signal properly aligned into monochromator the only remaining procedure before beginning image acquisition is the calibration of the coupling between the microscope and the monochromator. Calibration of the Raman microscope is very similar to procedures used to calibrate other Raman spectrometers. It is important to properly calibrate any instrument so as to be able to have trust in any data obtained from that instrument. The calibration of the Raman microscope has two parts, calibration of the monochromator based on a room light spectrum and calibration of the microscope based on a Raman standard.

Calibration of the instrument with the room light is done first to verify that detector and spectrometer are properly aligned. To accomplish this, place a fluorescent lamp above the entrance slit of the monochromator. In the Andor dashboard software set the slit width to 10 μm and the acquisition time to 0.5 seconds. Do not set the acquisition time to more than 1.0 seconds because the detector is very sensitive and at longer

exposure times the detector can become saturated with signal. Set the grating angle so that the detected region includes the 404.2 nm and the 435.83 nm lines from a fluorescent light. Acquire a spectrum, and in the software select *Manuel X-Calibration*. Select the 404.2 nm peak and assign it its correct wavelength and do the same for the 435.83 nm peak. Select the *Quadratic Polynomial Fit* and select *Apply to all New Acquisitions*. Reacquire an additional spectrum of the light to verify that the manual calibration worked correctly. Once this calibration step is verified, remove the lamp. Place the black box, which was built to prevent stray light from entering the monochromator, over the collection optics.

While the first calibration step ensures that the detector and monochromator are properly aligned, the second calibration step is to ensure that the Raman microscope itself can properly collect Raman scattered light from a known reference standard. The known reference standard used in this calibration step is naphthalene.²⁷ First place immersion oil on the 100X objective and place a clean coverslip on the microscope stage. Place a small crystalline sample of naphthalene on the coverslip and bring the immersion oil into contact with the coverslip. Turn the laser on and look through the eye pieces to verify that the laser is properly focused onto the coverslip. Move the microscope stage so that the crystalline naphthalene is positioned above the laser on the microscope stage. Turn the *Path Control* knob; this controls the direction of the transmitted beam, from the eye piece direction to the side port direction and switch off the condenser light. In the Andor dashboard software set the slit width to 10 μm , the acquisition time to 20.0 seconds, and set the 1200 groove/mm grating to cover a Raman shift range of 750 to 1400 cm^{-1} .

Acquire a spectrum from naphthalene and verify that the peak positions and peak heights all correspond to the published reference spectrum.^{27, 40}

Figure 3.16 shows the reference Raman spectrum of naphthalene and the Raman spectrum of naphthalene obtained using the Raman microscope with the 600 groove/mm grating of the monochromator. If the peaks are not at the correct wavenumbers select **Manual X-Calibration** and select the peaks and type in the correct Raman shift. Select **Cubic Polynomial Fit** and then select **Apply to all New Acquisitions**. If a spectrum does not show up, recheck the alignment of the detection optics to ensure that nothing is blocking the collected signal from reaching the monochromator. If a manual calibration was required after acquiring a spectrum of naphthalene, acquire a second spectrum to verify the correct placement of the spectral peaks. A correct Raman spectrum of naphthalene using the 1200 groove/mm grating is shown in Figure 3.17.

3.4 – Point Illumination Imaging Procedure

Point illumination is an imaging technique where by the image of a sample is recreated point by point by coordinating a spectrum of the sample with the position of the microscope stage at the point when spectrum was obtained. A series of spectra are recorded in a raster pattern and the position of the stage when these spectra are obtained is recorded consecutively. The change in intensity of a spectral peak is used to provide the necessary contrast needed to visualize the sample being investigated. The position of the microscope stage at each data point allows for the spectra to be placed in the proper position in an image grid.

Imaging a sample by point illumination is fairly simple to perform; however, it should be noted it is time consuming. To start the point illumination imaging procedure,

the sample must first be loaded onto a clean cover slip and the laser must be brought into focus onto the sample. Select the point where the image is to begin, this will be the starting point for the raster scan. Turn on the digital read out if it is not already displaying the relative position of the microscope. Open and run the *Microscope Coordinate Control* program as described in Appendix A. Zero the digital read out for this first data point, and verify that the LabVIEW program is displaying a zero reading for both the X and Y positions.

Acquire a spectrum of the sample surface and record the position reading for this, the first data point. Once this spectrum is acquired, move the microscope stage to the next position following the raster scan pattern shown in Figure 2.3. Acquire the second spectrum of the sample surface and take the second position reading for this, the second data point. Continue this process following the raster scan pattern in Figure 2.3 until enough data points have been obtained to fully map out the sample surface and its background coverslip surface. With all of the sequential spectral data and the microscope positions, an image of the sample can be recreated using the Igor Pro program described in Appendix B. The time consuming nature of this process becomes readily apparent when you consider that many samples require acquisition times in the neighborhood of hundreds of seconds for a single spectrum. The image acquisition time increases exponentially compared to a single acquisition because a single image consists of hundreds of data points.

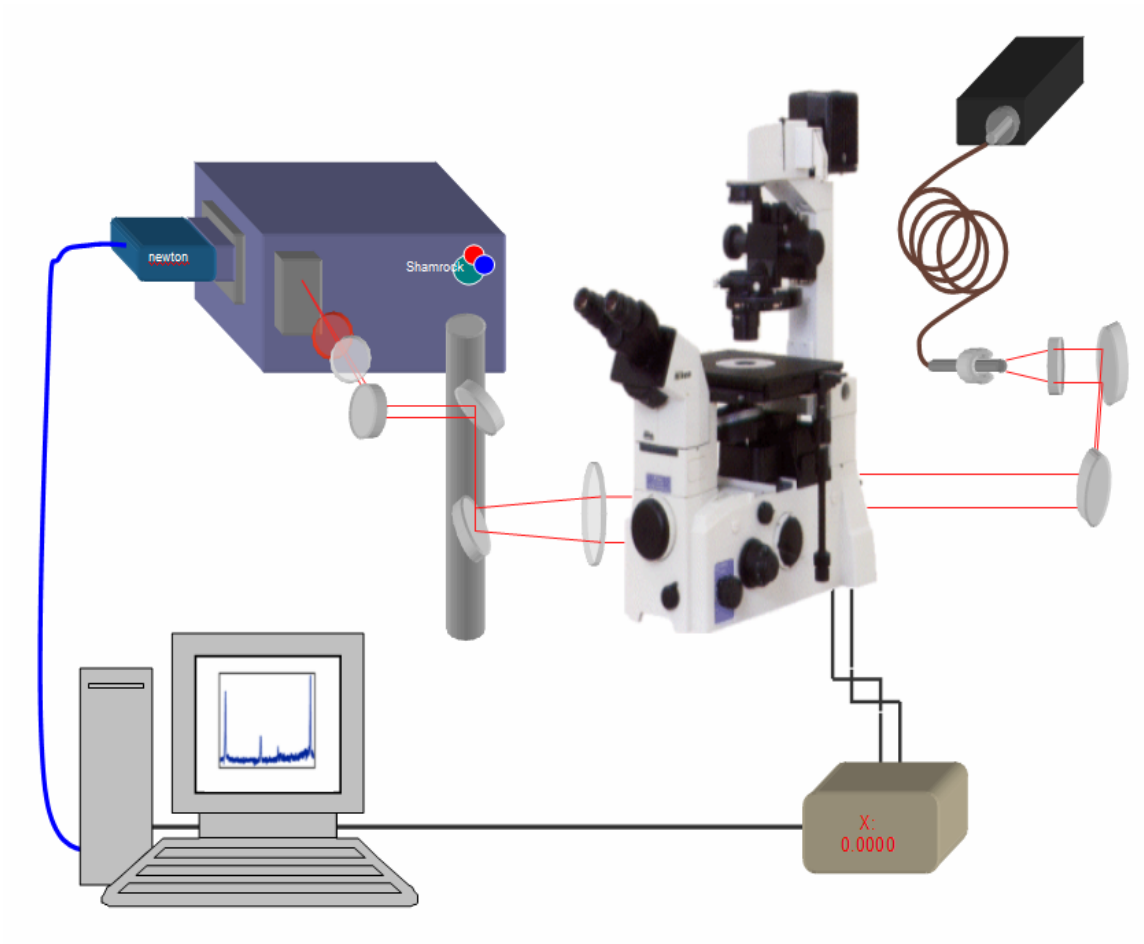


Figure 3.1: Schematic of the Raman microscope set-up.

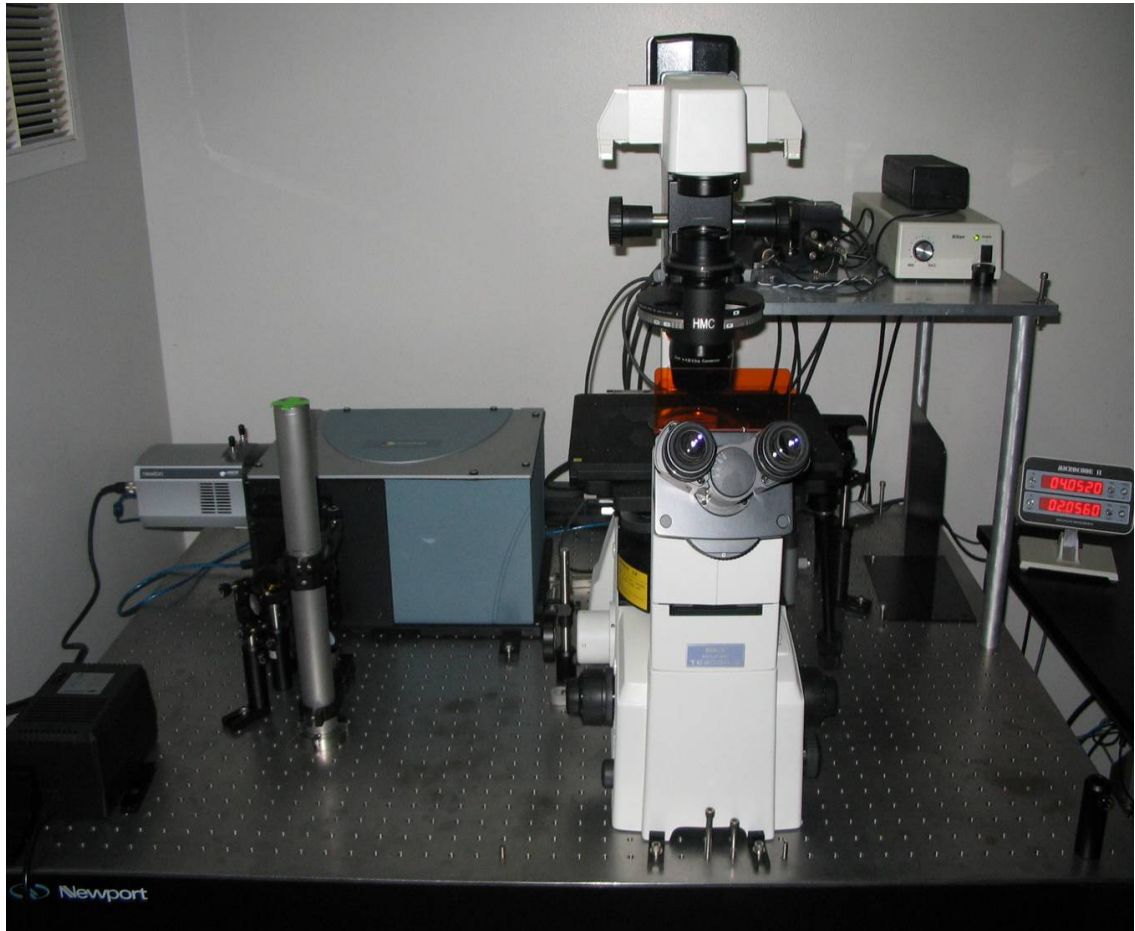


Figure 3.2: *Photograph of the Raman microscope set-up.*

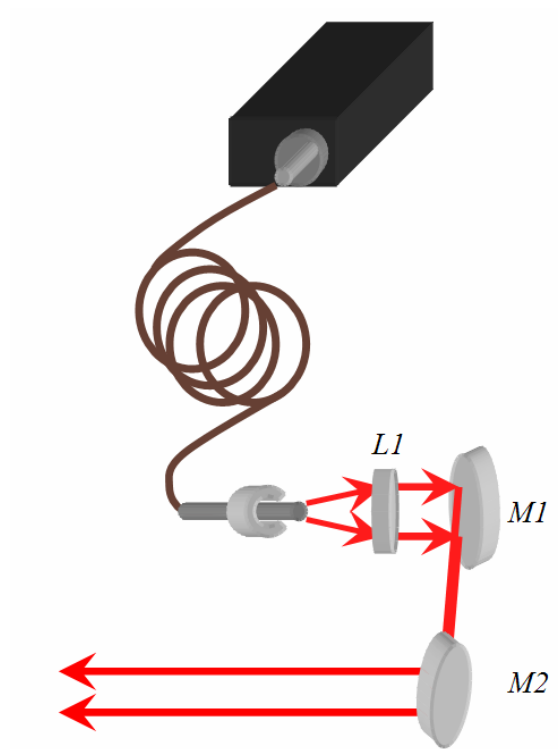


Figure 3.3: *Diagram of the laser excitation source and coupling optics used with the Raman microscope.*

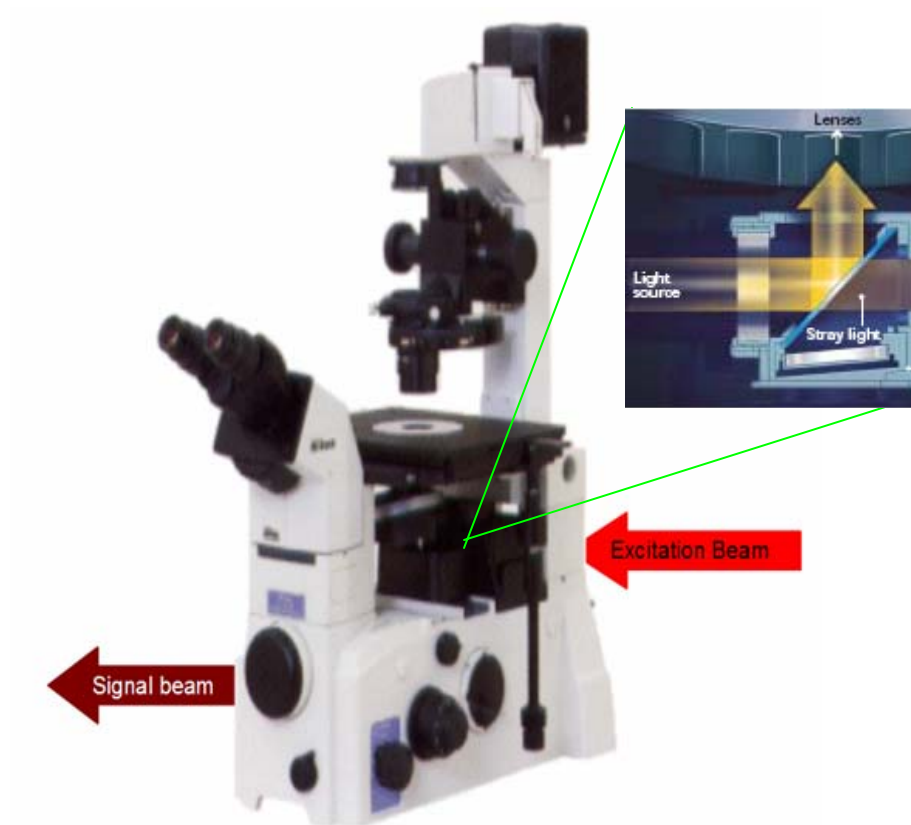


Figure 3.4: *The microscope used in the experimental setup and the direction of the signal and excitation beams. The inset picture shows the path of the light off of the dichroic mirror and into the objective.*

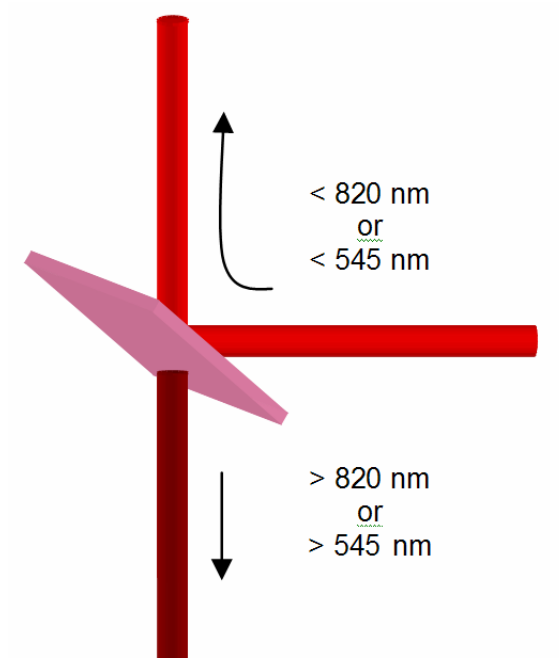


Figure 3.5: Schematic of the longpass dichroic mirrors used in the experimental setup.

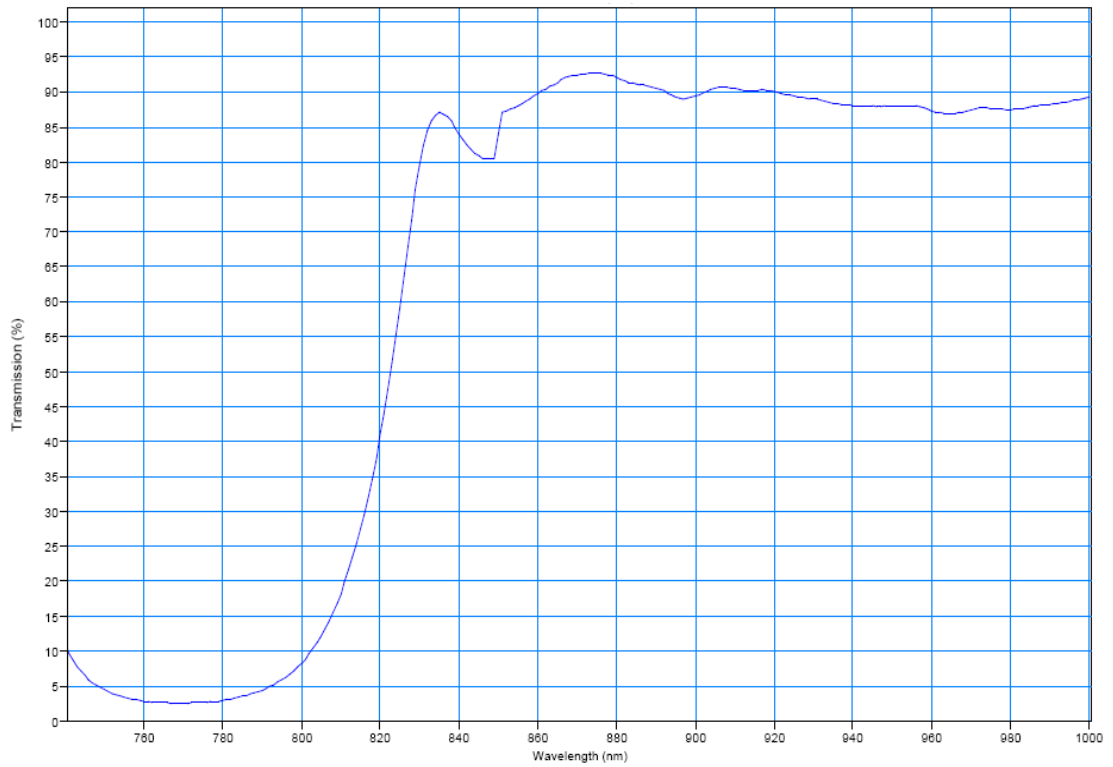


Figure 3.6: 820 nm DRLP transmission curve for the dichroic mirror used with 785 nm excitation light. This transmission curve was obtained via email correspondence with a representative from Omega Optical; a copy can be obtained from their website, www.omegafilters.com.

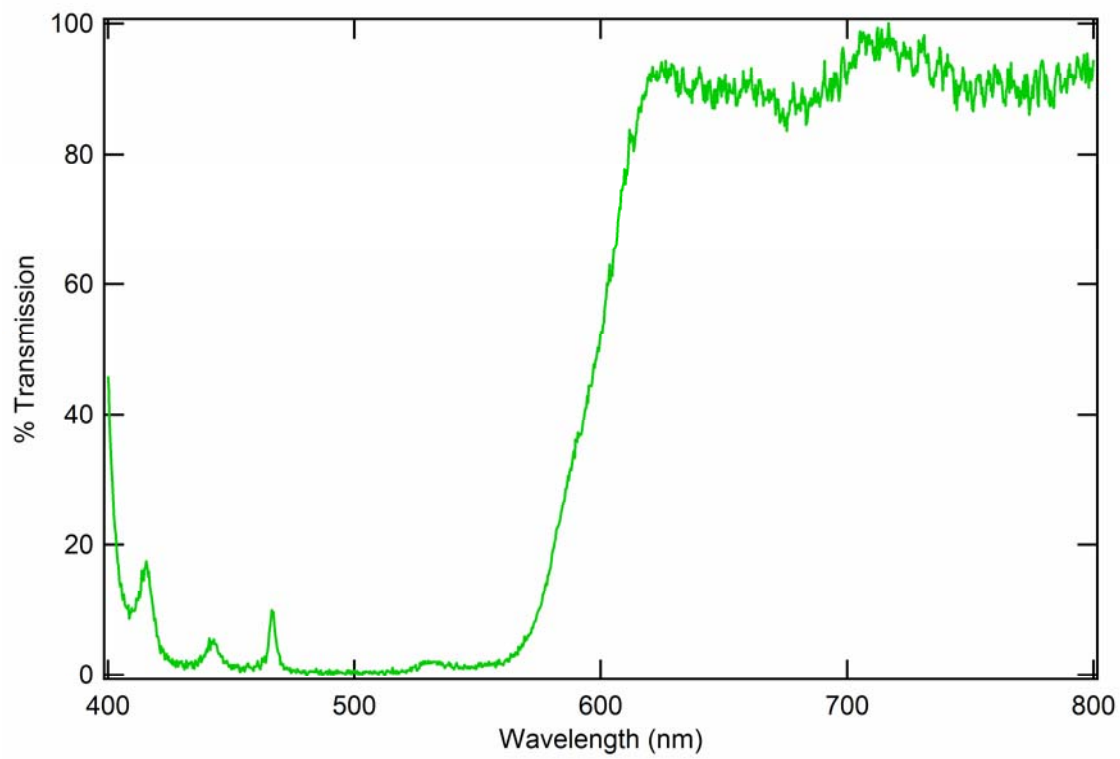


Figure 3.7: *The 545 nm DRLP transmission curve for the dichroic mirror used with the 532 nm excitation light.*

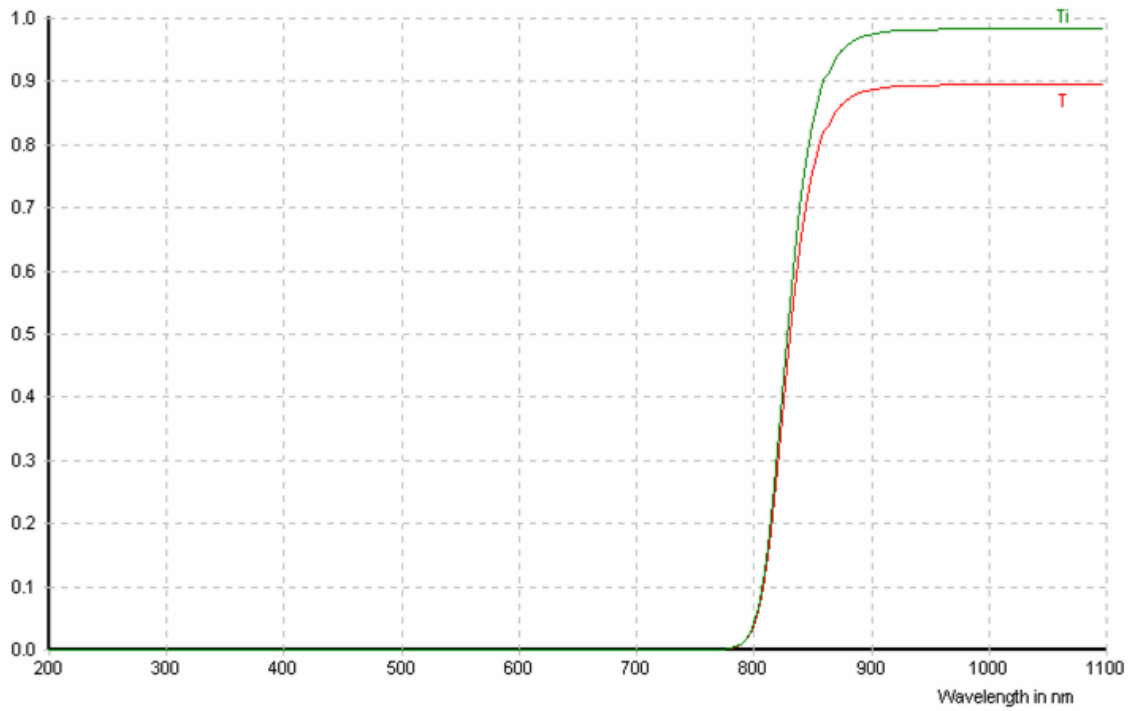


Figure 3.8: *The 830 nm red Schott glass interference filter transmission curve. This transmission curve was obtained from the Schott glass website, www.us.schott.com.*

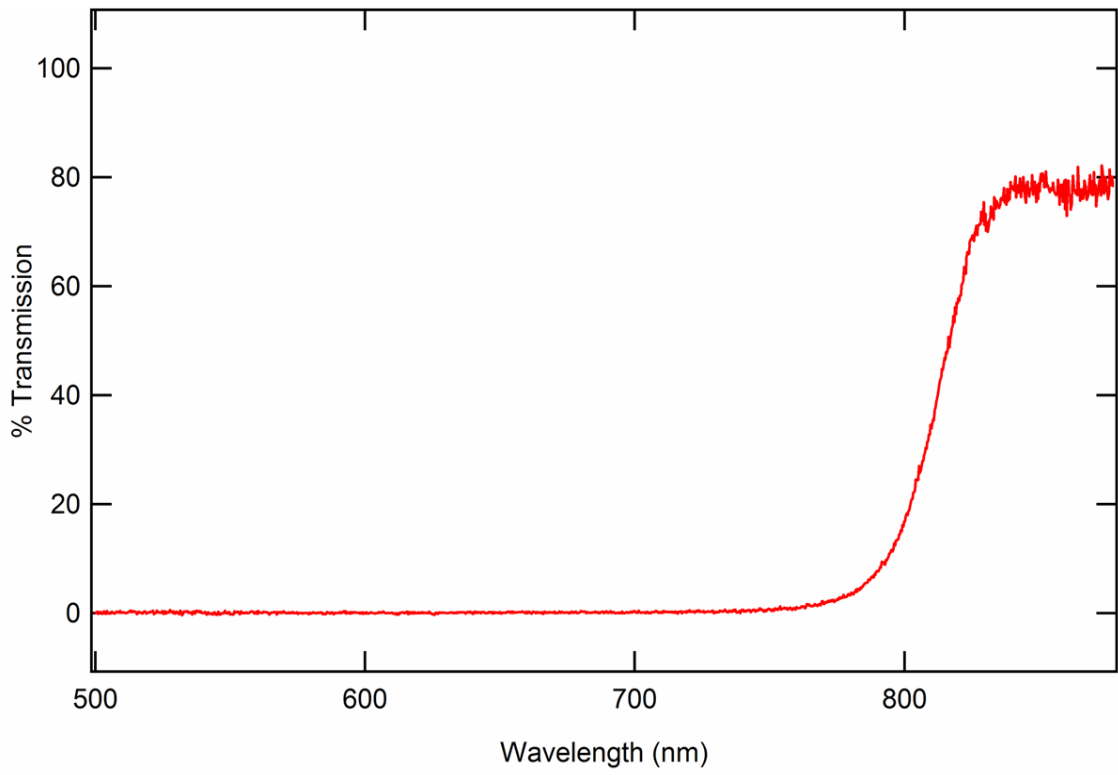


Figure 3.9: *The 800 nm longpass filter transmission curve.*

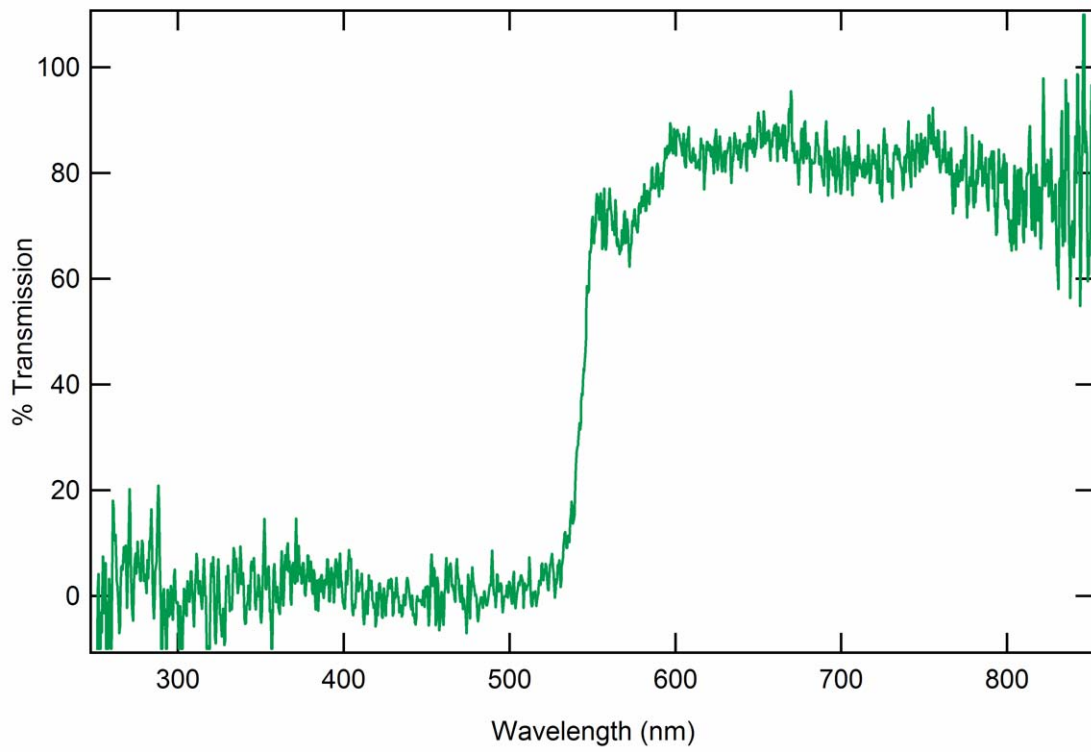


Figure 3.10: *Transmission curve of the 550 nm longpass filter.*

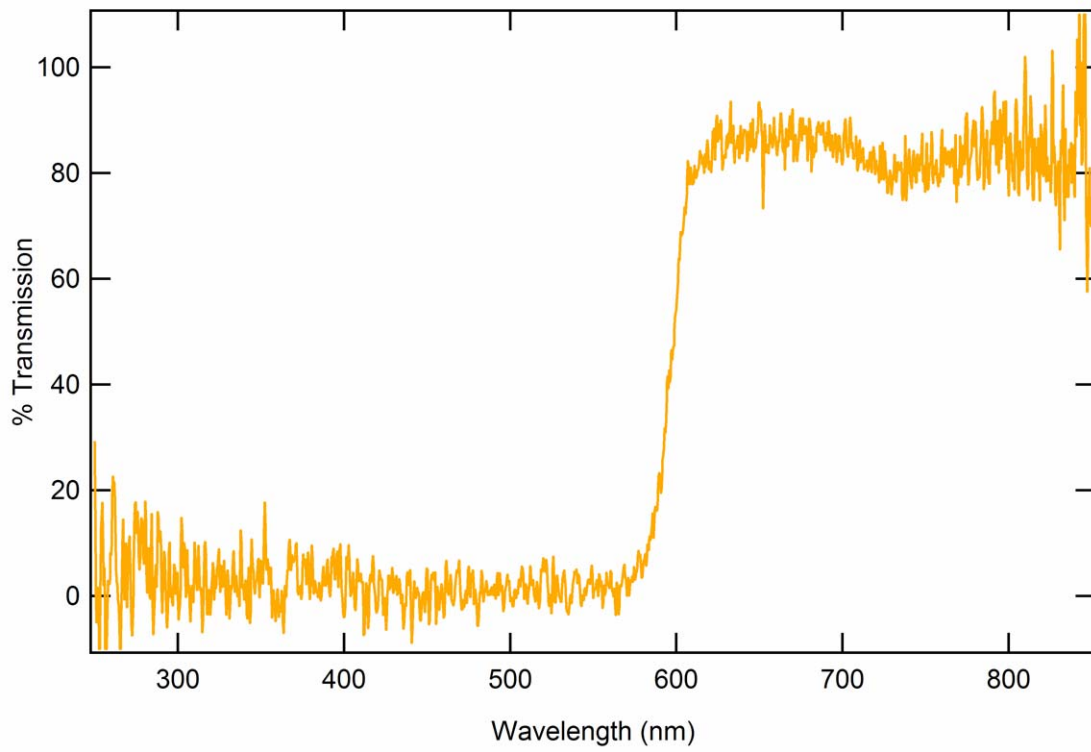


Figure 3.11: *Transmission curve for the 600 nm orange Schott glass interference filter.*

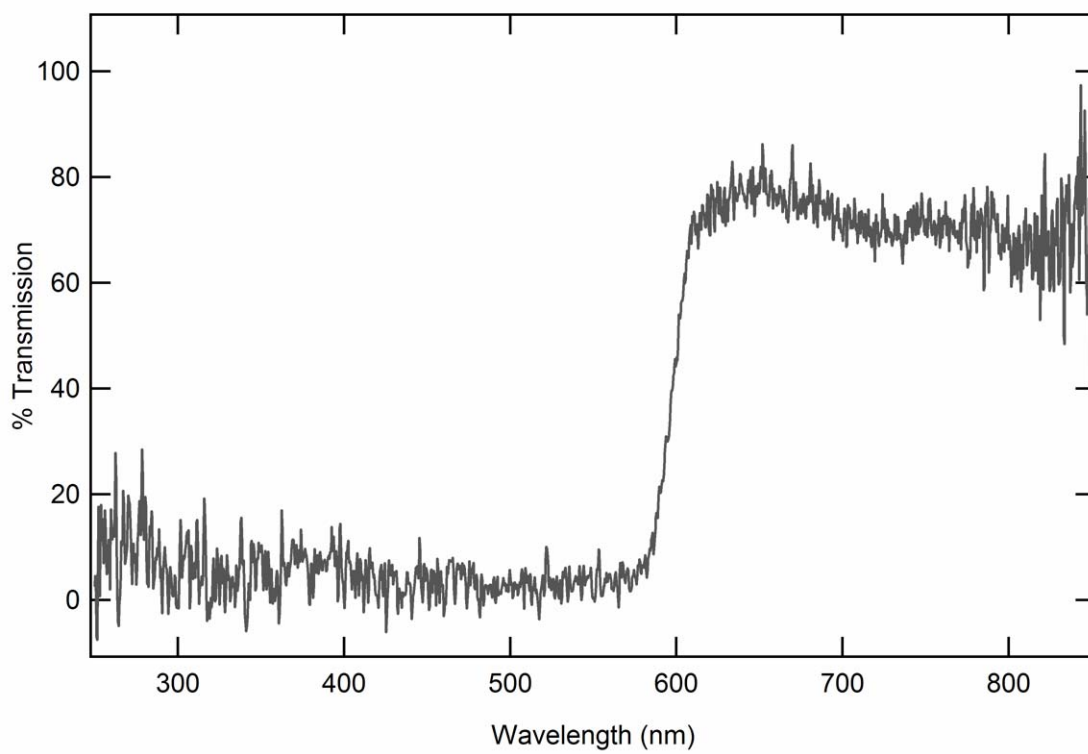


Figure 3.12: *Combined filter transmission curve when using 532 nm excitation.*

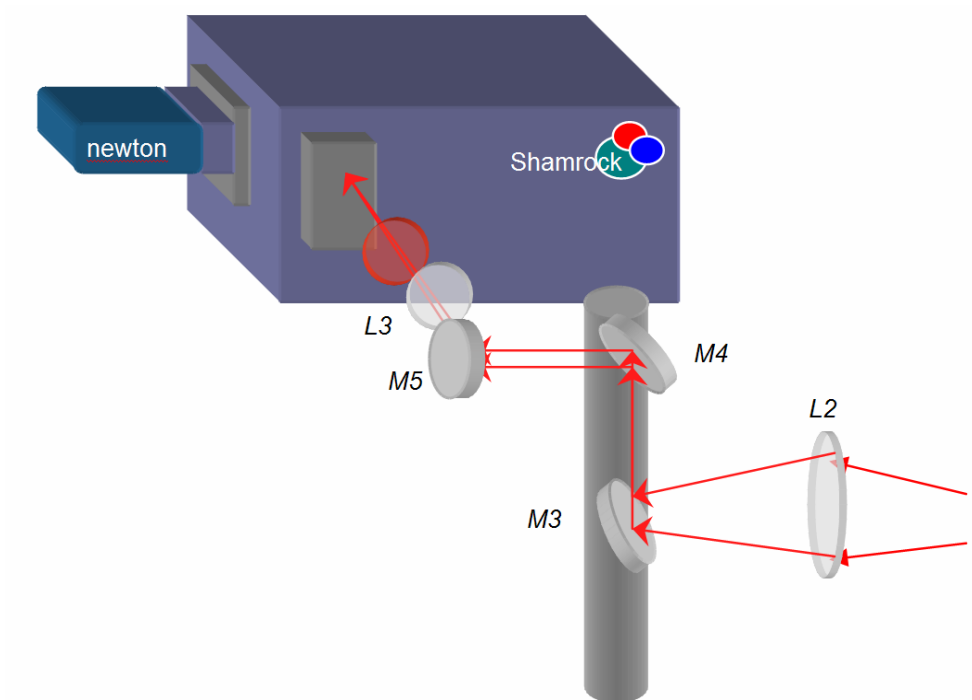


Figure 3.13: *The schematic for the signal collection and detection optics used in the experimental setup.*

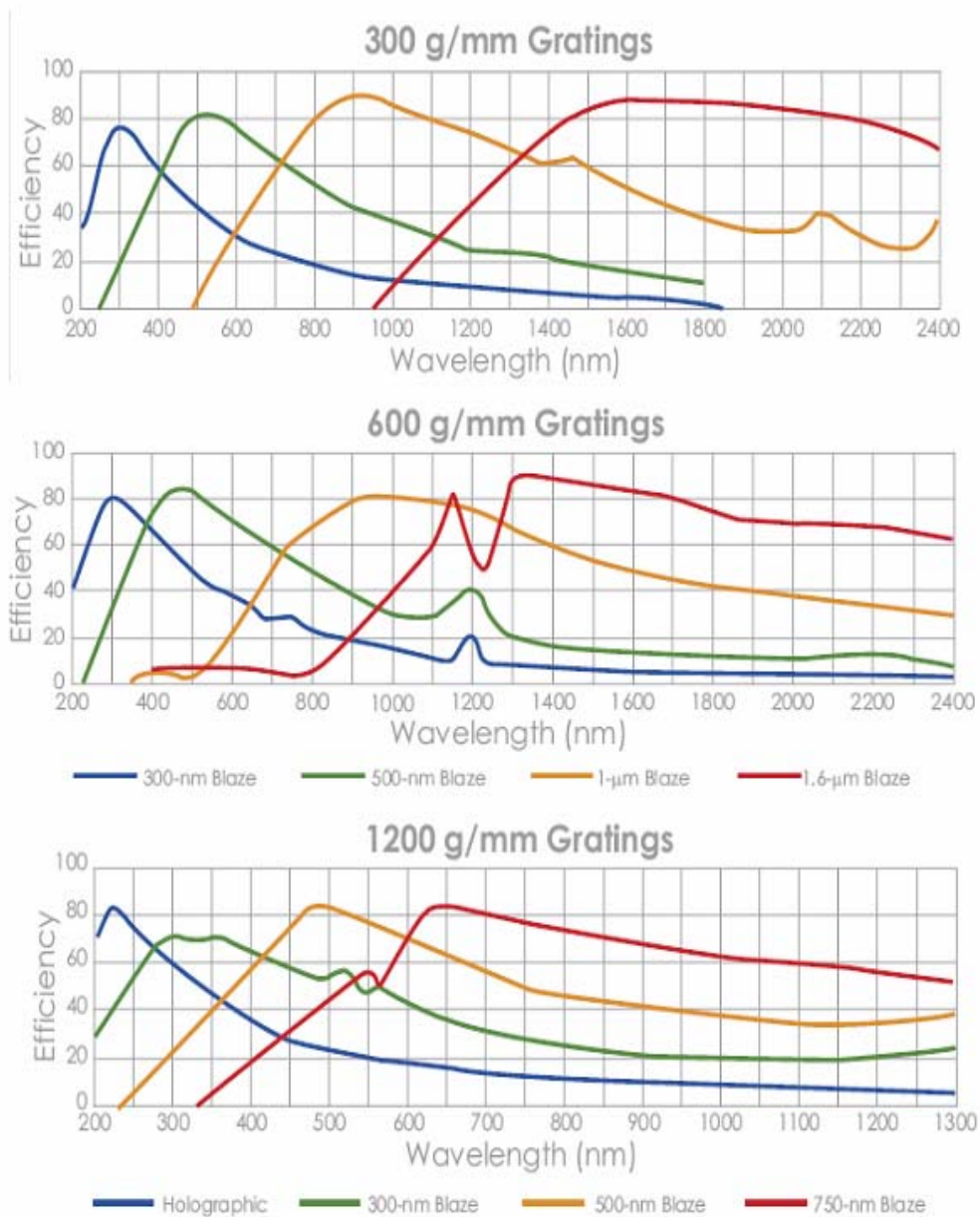


Figure 3.14: The grating efficiency curves for the diffraction gratings used in the monochromator. All grating efficiency curves can be seen in their original format at the Andor website, www.andor.com.

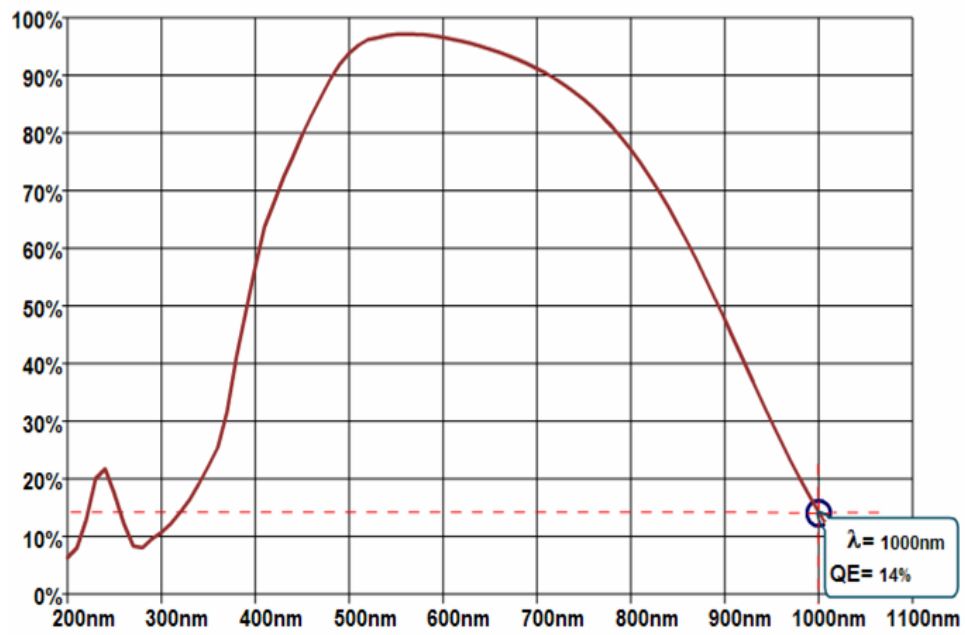


Figure 3.15: *The Andor EMCCD efficiency curve. The efficiency curves for Andor CCD devices can be found on their website, www.andor.com.*

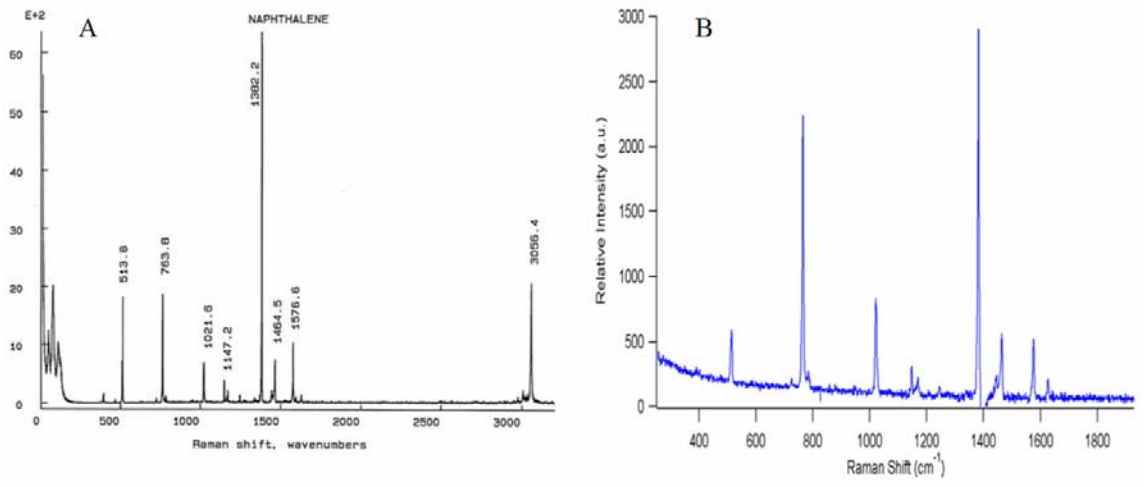


Figure 3.16: A) Reference Raman spectrum of naphthalene.^{27, 40} B) Raman spectrum of naphthalene obtained in this study

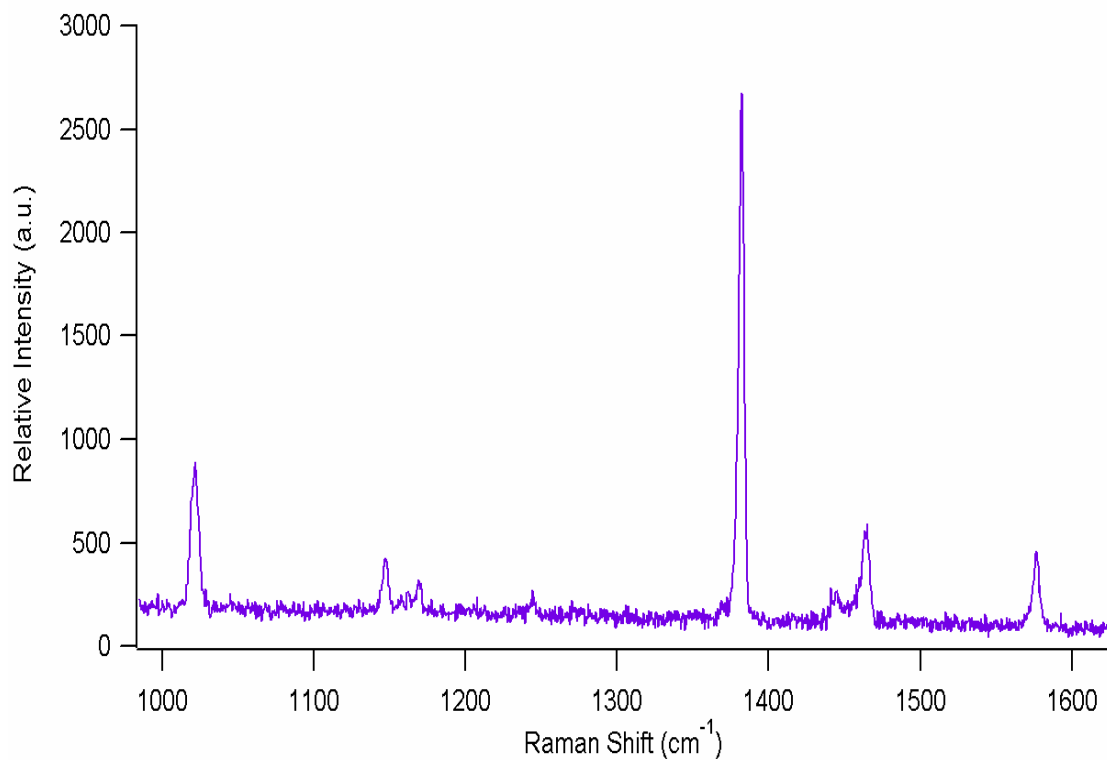


Figure 3.17: Raman spectrum of naphthalene acquired using the Raman microscope and a 1200 groove/mm grating and a 20 second exposure time.

Pin Number	Pin Name	Function	Signal Direction
1	DCD	Data Carrier Detected	Not Used
2	RXD	Receive Data	Data from Device to Computer
3	TXD	Transmit Data	Data from Computer to Device
4	DTR	Data Terminal Ready	Data from Computer to Device
5	GND	Signal Ground	Signal Ground
6	DSR	Data Set Ready	Data from Device to Computer
7	RTS	Request to Send	Not Used
8	CIS	Clear to Send	Data from Device to Computer
9	SEND	Ring Indicator	Data from Computer to Device

Table 3.1: *The pin configuration for the RS-232 cable connection used to connect the digital readout to the computer.*

CHAPTER 4

RESULTS AND CONCLUSIONS

4.1 – Introduction

The goal of building a Raman microscope is to be able to image multi-component systems. The ultimate goal is to spectroscopically image the domain formation of model lung surfactant systems. Before testing the feasibility of the Raman microscope to image complex mixtures, several different model systems were investigated. The model systems investigated included a macroscopic crystalline sample of a known Raman standard (naphthalene), a microscopic crystalline sample (d_{62} -DPPC), and homogeneously composed lipid (d_{62} -DPPC) vesicles. A model complex system was also investigated to test the feasibility of imaging a multi-component system. The model complex system was composed of crystalline naphthalene and palmitic acid. Palmitic acid and d_{62} -DPPC were specifically chosen because of their important role in lung surfactant research. All experiments were conducted at room temperature (~ 23 °C) and at atmospheric pressure.

4.2 – Imaging Macroscopic Crystalline Naphthalene

Before investigating heterogeneous samples it was necessary to first understand what to expect when imaging the individual components. The first sample to be imaged

with the Raman microscope was macroscopic sized crystalline naphthalene, C₁₀H₈. This sample was chosen as the first model system because the Raman spectrum of naphthalene is well known and can be obtained with relatively short acquisition times. The reason for first choosing a macroscopic sized sample is that it can be seen with the unaided human eye on the microscope coverslip. This is extremely useful in the verification of image recreation.

The NIR excitation source of 785 nm was used with the power set to 200 mW at the microscope objective. The power intensity of the focused laser spot was calculated to be 1.986 x 10⁶ W/cm². The power intensity of the laser spot focused by the 100X objective was calculated using Equation 4-1; where P is the power of the laser at the objective, λ is the wavelength of the excitation source in cm, f is the focal length of the objective lens in mm, and w_ℓ is the microscope objective aperture opening in mm.²⁸

$$I_o = \frac{0.68 \cdot P}{\lambda^2} \left(\frac{w_\ell}{f} \right)^2 \quad (4-1)$$

The Raman microscope was calibrated before beginning spectral acquisition as outlined in Chapter 3. Although the microscope coverslips are purchased “pre-cleaned”, further cleaning is done to further reduce surface contamination that might hinder image acquisition. Coverslips for these experiments were rinsed with ethanol and wiped clean with lint-free Kim wipes. The coverslips were then rinsed thoroughly with nanopure water (18 MΩ resistivity) and allowed to dry for 30 minutes in an oven at T > 100 °C.

A drop of type DF immersion oil was placed on the 100X microscope objective and a clean coverslip was placed on the microscope stage above the objective.

Crystalline naphthalene was obtained from Sigma Aldrich and used as received.

Macroscopic sized (2 mm to 250 μm) crystals of naphthalene were deposited at random on the coverslip. The sample was brought into proper focus and a sample area was selected to encompass one complete crystal and one partial crystal. The sample image size was determined to be 4 mm X 2 mm and a step size was set to 250 μm . The choice of step size was arbitrary and was chosen solely to provide an adequate number of data points for image reconstruction. 153 data points were obtained using the 250 μm step size and desired image size of 4 mm X 2 mm. The total image acquisition time was 3 hours using a CCD exposure time of 10 seconds per spectrum. The interference filter with a cut-on wavelength of 800 nm was used to filter out the excess incident 785 nm light.

The 1200 groove/mm diffraction grating was used for spectral acquisition. The grating was positioned to cover a spectral window of 832 nm to 882 nm. This spectral window corresponds to a Raman shift of 730 cm^{-1} to 1406 cm^{-1} . In this spectral window several Raman bands can be monitored, and specifically the C-H out-of-plane deformation mode at 763.5 cm^{-1} , the C-H in-plane deformation mode at 1022 cm^{-1} , and the C-C double bond stretching vibration at 1382 cm^{-1} . The entrance slit width of the monochromator was set to 100 μm . A series of background spectra of the clean coverslip were obtained before image acquisition began. A well defined background is extremely important to proper spectral acquisition because false spectral features appear as a result of scattering caused by the excitation source passing through several different media (Immersion oil and coverslip). Figure 4.1 shows the background spectrum of the coverslip, a raw naphthalene spectrum before background correction, and the final

background subtracted spectrum of naphthalene. Note that the broad spectral “bump” above 1100 cm^{-1} present in the background and raw spectra of naphthalene is removed by proper background subtraction in Figure 4.1.

Raman spectra of the coverslip were obtained in a raster pattern as outlined in Chapter 3, and the image reconstruction was conducted as outlined in Appendix B. The resulting images of the sample are shown in Figure 4.2. Image contrast is based on the presence of the Raman band at 763.5 cm^{-1} , which corresponds to the presence of the C-H out-of-plane deformation mode of naphthalene. Figure 4.2a shows the contour plot of the coverslip. Figure 4.2b shows the three-dimensional (3-D) Raman band intensity distribution of the C-H out-of-plane deformation mode on the surface of the coverslip. Figure 4.2c shows the false color image of the coverslip with the naphthalene crystals in blue (high to moderate Raman band intensity) and red (moderate to low Raman band intensity) and the background is in green (zero Raman band intensity). Figure 4.3a shows the Raman spectrum taken at point (1.75, 0.75), which corresponds to the presence of a high intensity Raman band. Figure 4.3b shows the Raman spectrum taken at point (1.0, 0.5), which corresponds to the presence of a moderate intensity Raman band. Figure 4.3c shows the Raman spectrum taken at point (3.5, 0.5), which corresponds to the absence of a Raman band, or the background.

4.3 – Imaging Microscopic d_{62} -DPPC Crystals

The second model system chosen for study with the Raman microscope was a microscopic ($< 250\text{ }\mu\text{m}$) sized sample. The first microscopic sized sample imaged was crystals of 1,2-dipalmitoyl- d_{62} -*sn*-glycero-3-phosphocholine (d_{62} -DPPC). Acyl-chain-deuterated 1,2-dipalmitoyl-*sn*-glycero-3-phosphocholine (d_{62} -DPPC) is a lipid used to

investigate domain formation in lung surfactant studies.⁴¹⁻⁴³ The CD₂ and CD₃ vibrational modes of *d*₆₂-DPPC allow this lipid to be distinguished spectroscopically in a mixture with other non-deuterated lipids. Powdered *d*₆₂-DPPC was obtained from Avanti Polar Lipids and was used without further purification.

The NIR 785 nm excitation source was used. The power was set at 200 mW before the microscope objective and the calculated power intensity of the focused spot was $1.986 \times 10^6 \text{ W/cm}^2$. A drop of type DF immersion oil was placed on the 100X microscope objective and a clean coverslip was placed on the microscope stage above the objective. Microscopic sized (100 μm to 10 μm) crystals of *d*₆₂-DPPC were deposited at random on the coverslip. The sample was brought into proper focus and a sample area was selected to encompass one isolated crystal. The sample image size was determined to be 60 μm X 50 μm and the step size was set to 5 μm . 143 data points were obtained using the 5 μm step size and the desired image size of 60 μm X 50 μm . A red Schott glass filter with a cut-on wavelength of 830 nm was used to filter out the excess incident 785 nm light.

The 1200 groove/mm diffraction grating was used for spectral acquisition. The grating was positioned to cover a spectral window of 914.17 nm to 962.57 nm. This spectral window corresponds to Raman shifts of approximately 1800 cm^{-1} to 2350 cm^{-1} when using 785 nm light as the excitation source. In this spectral window several Raman bands can be monitored, specifically the CD₃-symmetric stretch (SS) at 2075 cm^{-1} , the CD₂-SS at 2105 cm^{-1} , the CD₂-asymmetric stretch (AS) at 2195 cm^{-1} and the CD₃-AS at 2220 cm^{-1} .⁴¹ The entrance slit width of the monochromator was 200 μm . The total image acquisition time was 12 hours using a 200 second CCD exposure time per

spectrum. The reason for the long exposure time is that the CCD quantum efficiency is very low (< 35%) at these wavelengths and longer exposure times are needed to obtain a spectrum with an adequate signal-to-noise ratio.

The d_{62} -DPPC crystal imaged measured approximately 35 μm in diameter and was roughly circular in shape. Figure 4.4a shows the bulk Raman spectrum of crystalline d_{62} -DPPC, and Figure 4.4b shows the spectrum of a crystal of d_{62} -DPPC taken with the Raman microscope. The two spectra match up exactly as expected with only the peak intensities being different due to the lack of number density in the micro-Raman spectrum compared to the bulk Raman spectrum. The image of the d_{62} -DPPC crystal was based on the presence or absence of the CD₂-SS at 2105 cm^{-1} . Figure 4.5a shows the contour plot of the crystal of d_{62} -DPPC with the purple color representing the background, or zero Raman band intensity, and red representing a maximum intensity. Figure 4.5b shows the 3-D Raman band intensity distribution of the CD₂-SS on the surface of the coverslip. Figure 4.5c is a false color image of the d_{62} -DPPC crystal with purple representing the background (i.e. no CD₂-SS present), and red the maximum intensity.

4.4 – Imaging Microscopic Homogeneous d_{62} -DPPC Vesicles

The third model system studied with the Raman microscope was chosen to be a non-crystalline microscopic sample. The system chosen to be studied with the Raman microscope were vesicles made of 1,2-dipalmitoyl- d_{62} -sn-glycero-3-phosphocholine (d_{62} -DPPC). Lipid vesicles are frequently used as model systems to investigate lipid structure formation in liquids to study cellular structures and components. The hydrophobic tails of lipids form bilayers in the presence of water to form cell like (i.e.

spherical) structures. Powdered d_{62} -DPPC was obtained from Avanti Polar Lipids and used without further purification. The procedure for making vesicles from d_{62} -DPPC was also obtained from Avanti and used without modification. To make the vesicles 40 μg of d_{62} -DPPC was measured into a volumetric flask and 25 mL of nanopure water was added. This mixture is then heated above the phase transition temperature of 53 $^{\circ}\text{C}$ with constant stirring for one to two hours. The vesicles formed under these conditions ranged in size from approximately 10 μm to 200 μm in diameter. The size range of the vesicles was verified by examining the vesicles suspension with the microscope set to view in the bright field mode.

The NIR 785 nm excitation source nm was used with the power set to 200 mW before entering the microscope objective with the same calculated power intensity of $1.986 \times 10^6 \text{ W/cm}^2$. A drop of type DF immersion oil was placed on the 100X microscope objective and a clean coverslip was placed on the microscope stage above the objective. A 20 μL droplet of the d_{62} -DPPC vesicle suspension was deposited on the coverslip. Because of the low quantum efficiency of the detector for the signal wavelengths and the requisite long exposure times, the excess water from the vesicle solution was allowed to evaporate before image acquisition began. If the vesicles dehydrated during image acquisition this could cause changes in the image over time. The sample was brought into proper focus and a sample area was selected to encompass several vesicles. The sample image size was determined to be 150 μm X 100 μm and the step size was set to 10 μm . 176 data points were obtained using the 10 μm step size and the desired image size of 150 μm X 100 μm . The total image acquisition time was 15 hours using a 240 second CCD exposure time per spectrum. A red Schott glass filter

with a cut-on wavelength of 830 nm was used to filter out the excess incident 785 nm light.

The 1200 groove/mm diffraction grating was used for spectral acquisition. The grating was positioned to cover a spectral window of 914.17 nm to 962.57 nm. This spectral window corresponds to Raman shifts of approximately 1800 cm^{-1} to 2350 cm^{-1} when using 785 nm light as the excitation source. In this spectral window several Raman bands could be monitored, specifically the CD_3 -symmetric stretch (SS) at 2075 cm^{-1} , the CD_2 -SS at 2105 cm^{-1} , the CD_2 -asymmetric stretch (AS) at 2198 cm^{-1} and the CD_3 -AS at 2220 cm^{-1} .⁴¹ The entrance slit width of the monochromator was set at $200\text{ }\mu\text{m}$.

The d_{62} -DPPC vesicles imaged ranged in size from approximately $10\text{ }\mu\text{m}$ to $50\text{ }\mu\text{m}$ in width. The vesicles were roughly circular or oval in shape. The image of the d_{62} -DPPC vesicles was based on the presence or absence of the CD_2 -SS Raman band at 2105 cm^{-1} . Figure 4.6a shows the contour plot of several d_{62} -DPPC vesicles. The purple color represents the background, or zero Raman band intensity, and red represents the maximum Raman band intensity. Figure 4.6b displays the 3-D Raman band intensity distribution of the CD_2 -SS on the surface of the coverslip. Figure 4.6c is a false color image of the d_{62} -DPPC vesicles where purple is the background intensity (i.e. no CD_2 -SS present) and red is the maximum intensity. A spectrum of no Raman band intensity is shown in Figure 4.7a, and a spectrum of high Raman band intensity is shown in figure 4.7a, both of which were used to reconstruct the image of the d_{62} -DPPC vesicles.

4.5 – Imaging Microscopic Heterogeneous Crystalline Samples

The final model system studied with the Raman microscope was chosen to test the ability of the Raman microscope to spectroscopically image a heterogeneous sample.

Ideally a spectroscopic imaging device should display the ability to obtain an image from samples that are spatially separated, as well as spectrally separated. The system chosen to be studied was a mixture of microscopic sized crystalline naphthalene and palmitic acid (PA) spread on a microscope coverslip. The C-H stretching vibration of naphthalene at 3056 cm^{-1} and the CH_2 -AS of PA at 2880 cm^{-1} were chosen to indicate the presence of each compound.

Naphthalene and PA were obtained from Sigma Aldrich and used without further purification. Microscopic crystals of PA and naphthalene were created by crushing the two compounds together. The samples of naphthalene were placed in a freezer for 30 minutes before being crushed. This was done to ensure that the resulting samples would not melt after being crushed and exposed to the atmosphere. Once a microscopic sized crystalline mixture of both PA and naphthalene was created, both were blown onto a clean microscope coverslip. This resulted in a completely random distribution of each compound on the coverslip, as well as a random size distribution.

The visible 532 nm excitation source was used with the power set to 100 mW before the microscope objective with a calculated power intensity of $2.162 \times 10^6\text{ W/cm}^2$ at the center of the focused laser spot. The reason for using a lower power is that the 532 nm light focuses to a smaller spot diameter which results in higher power intensity. A drop of type DF immersion oil was placed on the 100X microscope objective. The coverslip with randomly distributed PA and naphthalene crystals was placed on the stage and the 100X objective was brought into focus. Several background spectra at different points, where no sample was present, were taken of the coverslip to ensure that the

background spectrum was well defined. These background spectra were averaged and later subtracted from all signal spectra as outlined in Appendix B.

The sample image size was determined to be 30 μm X 25 μm so as to encompass several crystals of PA and one crystal of naphthalene. 806 data points were obtained using a 1 μm step size for the desired image size of 30 μm X 25 μm . The total image acquisition time was 22 hours using a 20 second CCD exposure time per spectrum. A 550 nm longpass filter and an orange Schott glass filter with a cut-on wavelength of 600 nm were used in combination to filter out excess 532 nm light.

The 1200 groove/mm diffraction grating was used for the spectral acquisition. The grating was positioned to cover a spectral window of 602.52 nm to 649.48 nm. This spectral window corresponds to Raman shifts of approximately 2200 cm^{-1} to 3400 cm^{-1} when using 532 nm light as the excitation source. In this spectral window the Raman band at 3056 cm^{-1} corresponding to the C-H stretching vibration of naphthalene was monitored. The $\text{CH}_2\text{-SS}$ at 2850 cm^{-1} and the $\text{CH}_2\text{-AS}$ at 2880 cm^{-1} of PA were also monitored.⁴⁴ The entrance slit width on the monochromator was 200 μm .

The PA crystals imaged ranged in width from approximately 17 μm to 50 μm . The fully resolved image of a PA crystal was 17 μm wide. The 50 μm crystal was only partially imaged due to image size and time constraints. The naphthalene crystal imaged was approximately 15 μm wide. The images acquired were based on the presence of either the 3056 cm^{-1} Raman band indicative of naphthalene or the 2880 cm^{-1} Raman band indicative of PA. Figure 4.8 shows the bulk Raman spectrum of the coverslip covered with crystalline naphthalene and palmitic acid. Figure 4.8 demonstrates why a Raman microscope is needed to spatially differentiate components of a heterogeneous sample

that are in close proximity of each other. Taken as a whole, the Raman spectrum of the coverslip shows spectral contributions from both PA and naphthalene. Using the Raman microscope to spatially separate the samples into microscopic sized areas allows for the spectral contribution of each compound at one distinct point on the coverslip to be known.

Figure 4.9 shows the contour plot of the imaged area. Figure 4.9a shows the contour plot of the imaged area considering only the 3056 cm^{-1} C-H stretch of naphthalene. Figure 4.9b shows the contour plot of the imaged area considering only the 2880 cm^{-1} CH₂-AS. As can be seen from the comparison between the Figures 4.9a and b, the crystals are in deed spatially separated. Figure 4.9c is the combination of the two preceding contour plots with the naphthalene crystal in white and the palmitic acid crystals in black. The background (no spectral intensity) is colored grey. In Figure 4.9c the peak area, or spectral intensity, of naphthalene was scaled down by a factor of 10 so as to not dwarf the spectral intensity of PA. The scaling factor was calculated by dividing the largest peak area of naphthalene by the largest peak area of PA.

Figure 4.10 shows selected spectra collected along the red line of the contour plot. The red line represents the Y=8 μm line. As can be seen from the spectrum at the point (0, 8) there is no spectral intensity, confirming that this position is free of any crystalline material. This absence of spectral intensity confirms the background position. As the line progresses from point (0, 8) through point (10, 8) the Raman band at 3056 cm^{-1} increases and then decreases to zero intensity. This is indicative of the presence of a resolved portion of crystalline naphthalene. As the line progresses from the point (10, 8) to point (23, 8) the Raman band at 2880 cm^{-1} is observed to grow in spectral intensity and

then decrease to almost zero spectral intensity. This is indicative of the presence of a resolved portion of crystalline PA. As the line progresses past the point (23, 8) to point (30, 8) zero spectral intensity is maintained.

Figure 4.11 shows the 3-D Raman band intensity at the surface of the coverslip. Figure 4.11a shows the 3-D intensity distribution of PA at the surface of the coverslip based on the presence of the CH₂-AS at 2880 cm⁻¹. Figure 4.11b shows the 3-D intensity distribution of naphthalene at the surface of the coverslip based on the presence of the C-H stretching vibration at 3056 cm⁻¹. Figure 4.11c shows the combined 3-D spectral intensity distribution of both compounds at the surface of the coverslip. Again the spectral intensity of naphthalene was scaled down by a factor of 10 to prevent overwhelming the scale of PA. Figure 4.12 shows the false color image based the presence spectrally of naphthalene (white) and PA (black) on the surface of a microscope coverslip.

4.6 – Summary of Conclusions

The goal of this thesis work was to demonstrate that with specific modifications a spectroscopic imaging instrument, a Raman microscope, can be constructed from common laboratory inverted microscope and standard laser optics. The instrument shows the ability to perform all of the duties necessary for a spectroscopic imaging device. The Raman microscope was shown to accurately detect the correct Raman spectrum of known standards. The instrument also showed the ability to image several different types of samples of varying size and composition. The sample image size was also investigated and it was shown that the images obtained with the instrument for microscopic samples were as clear as images obtained from macroscopic samples.

The goal of the experiments performed with the Raman microscope was to demonstrate that the instrument could be used to reconstruct the images from spectral data for a variety of samples. All of the experiments conducted in this thesis work demonstrate that the Raman microscope can accurately recreate the image of the sample being analyzed. The simple compounds, both macroscopic and microscopic in size, that were studied demonstrate that the instrument can obtain the proper spectral data from a known location. The experiments also show that the ability of the instrument to image a sample is not limited by size, morphology, or chemical composition. The results of these experiments also show that the computer programs written to aid in image reconstruction can accurately take the acquired spectral data and combine it with the position data to visualize the sample.

The experiments with the model heterogeneous system demonstrated that the Raman microscope can spectrally distinguish between different compounds. The spectral resolution of the Raman microscope is dictated by the bandpass of the monochromator. With the slit width set to 200 μm and using the 1200 groove/mm grating, the bandpass varied between 15.334 cm^{-1} when analyzing the C-D stretching region ($\sim 2200 \text{ cm}^{-1}$) and 13.812 cm^{-1} when analyzing the C-H stretching region ($\sim 2900 \text{ cm}^{-1}$). The spatial resolution of the Raman microscope is dictated by the diameter of the focused laser spot (Equation 4-1) generated by the 100 X 1.3 NA oil immersion lens. When using 785 nm light for excitation the focused beam diameter is 3.32 μm and when using 532 nm light for excitation the focused beam diameter is 2.25 μm . These experiments also showed that the computer programs were able to utilize multiple spectral peaks for image reconstruction.

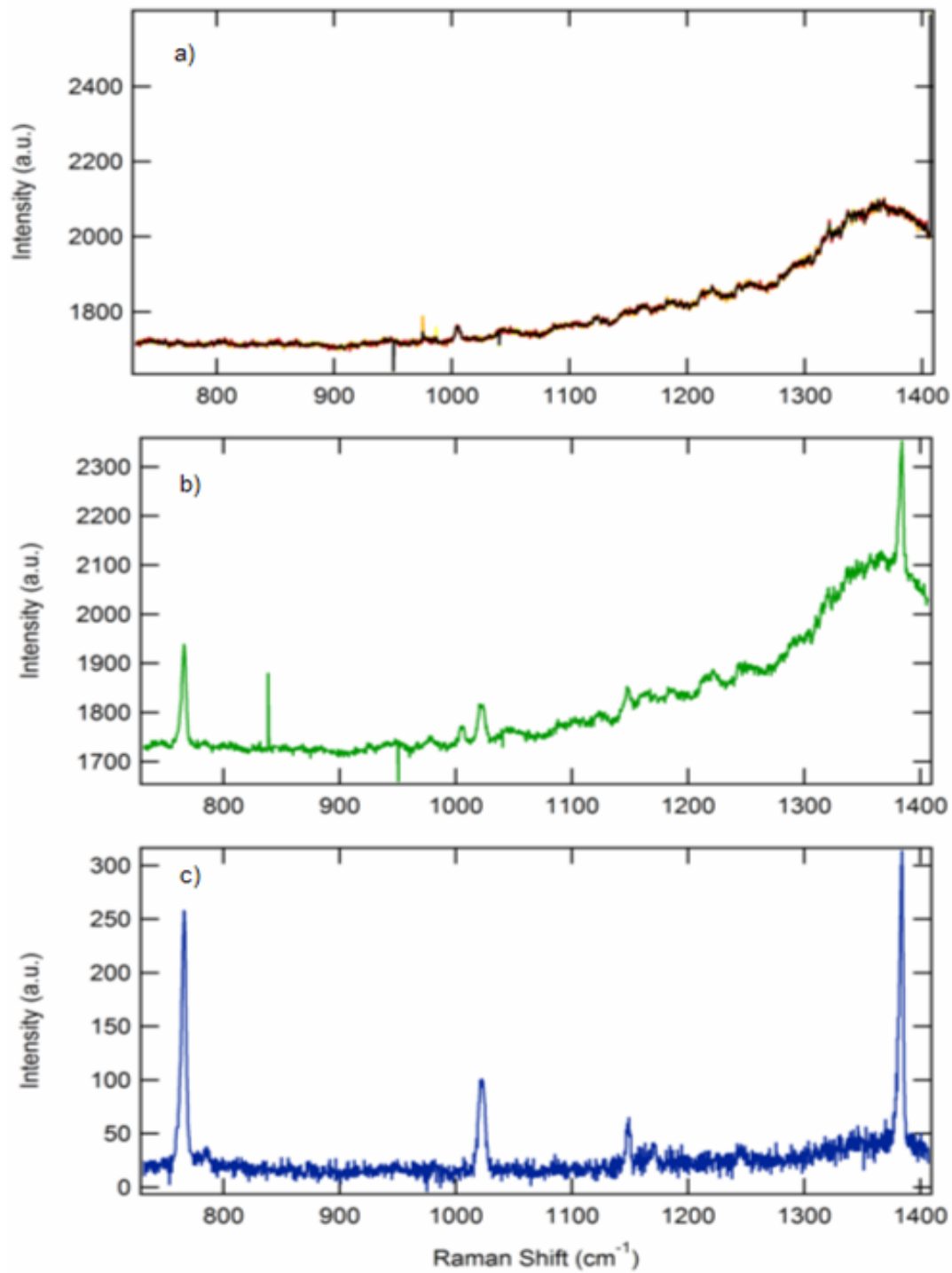


Figure 4.1: Spectra of a) microscope coverslip (background), b) raw naphthalene, and c) the background subtracted spectrum of naphthalene.

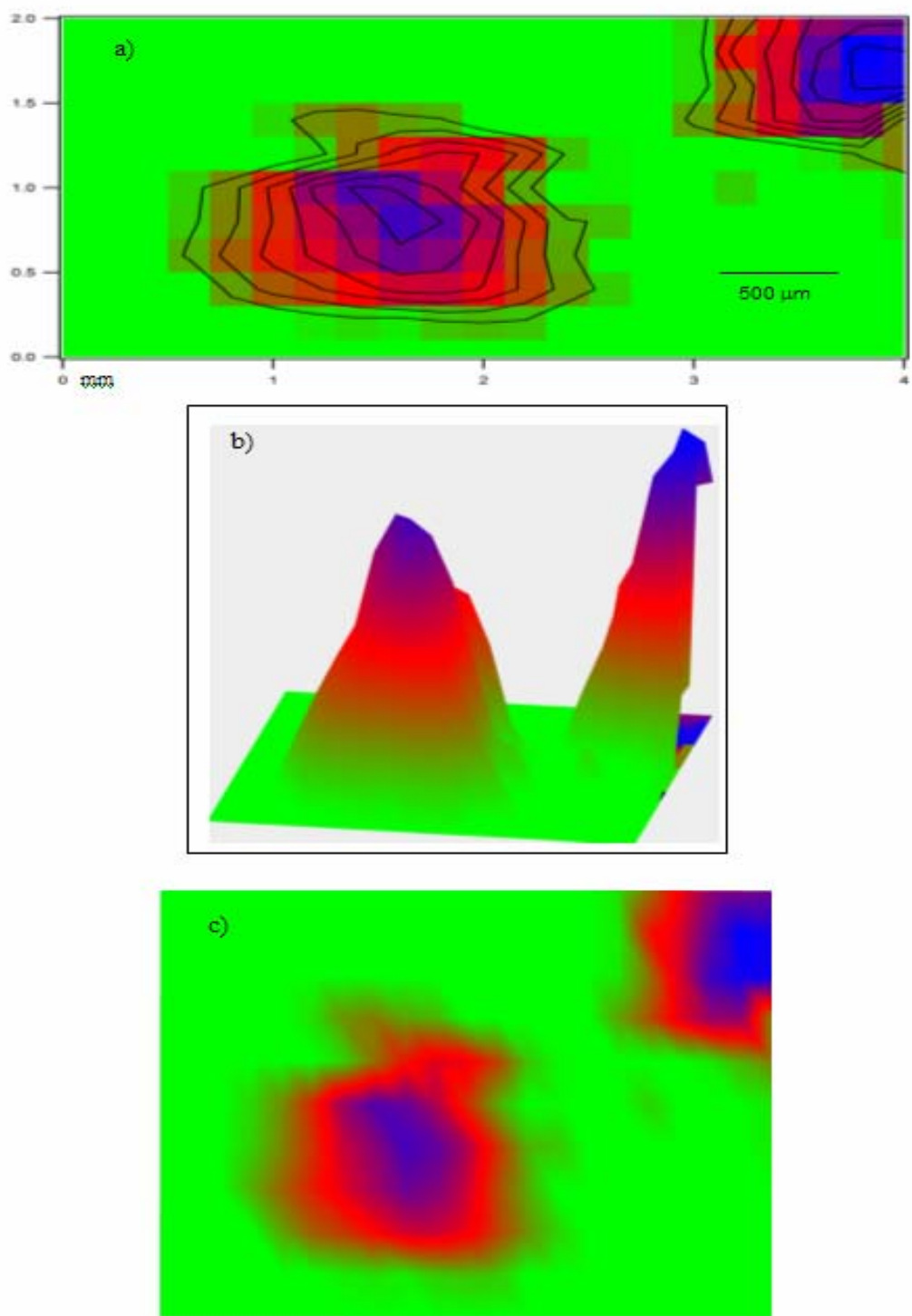


Figure 4.2: a) Contour plot of crystalline naphthalene on a coverslip. b) 3-D plot of the out-of-plane deformation intensity distribution of naphthalene on a coverslip. c) False color image of naphthalene on a coverslip.

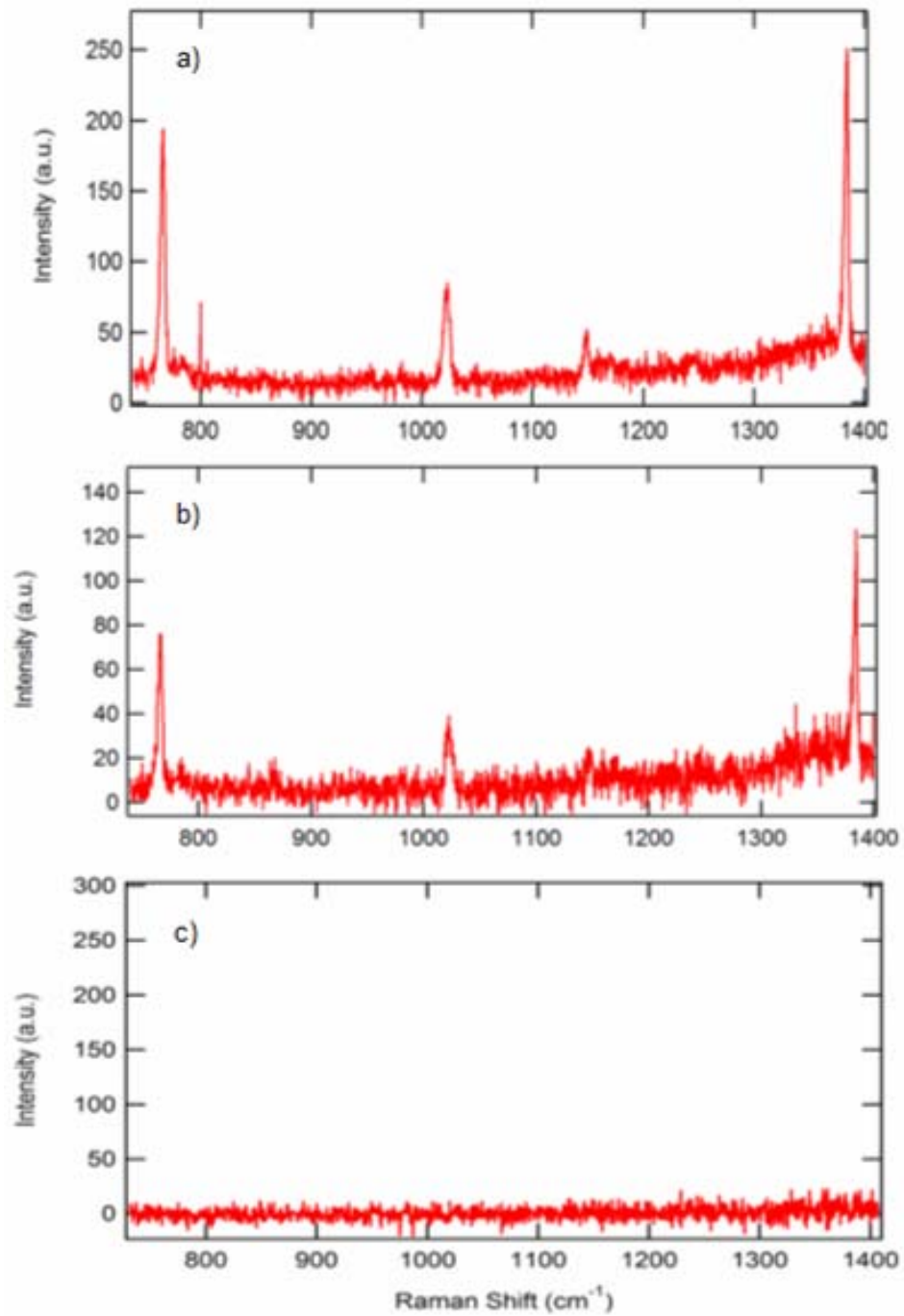


Figure 4.3: Selected Raman spectra taken at different points of the coverslip showing a) (1.75, 0.75) high intensity, b) (1.0, 0.5) moderate intensity, and c) (3.0, 0.5) no intensity

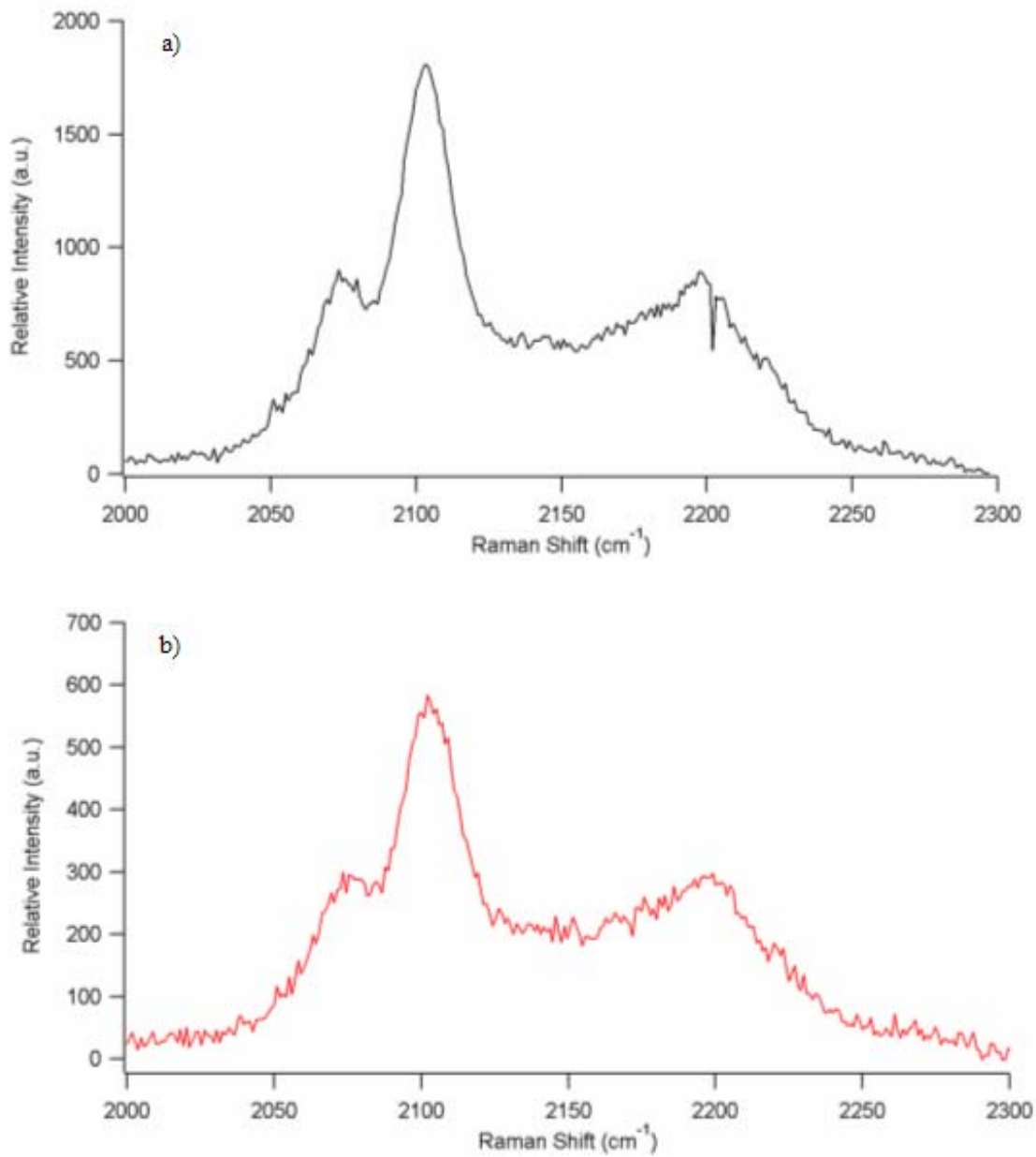


Figure 4.4: *a) Bulk Raman spectrum of d_{62} -DPPC using the RamanProbe™ fiber optic system. b) Micro-Raman spectrum of d_{62} -DPPC obtained using the Raman microscope.*

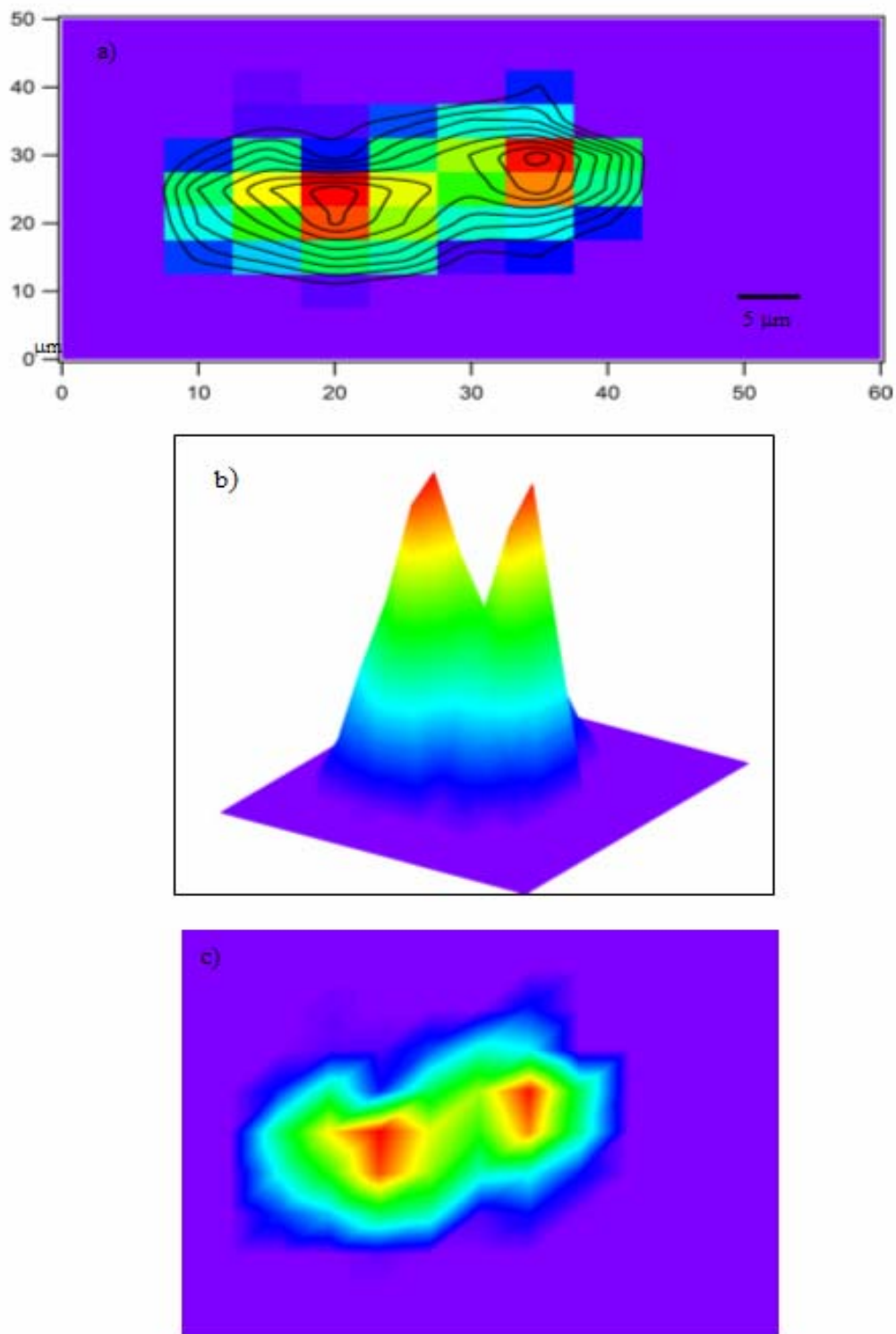


Figure 4.5: a) Contour plot of a d_{62} -DPPC crystal on the surface of a coverslip. b) 3-D plot of the $\text{CH}_2\text{-SS}$ (2105 cm^{-1}) intensity distribution of a d_{62} -DPPC crystal on the surface of a coverslip. c) False color image of the d_{62} -DPPC crystal based on the presence of the $\text{CH}_2\text{-SS}$ (at 2105 cm^{-1}).

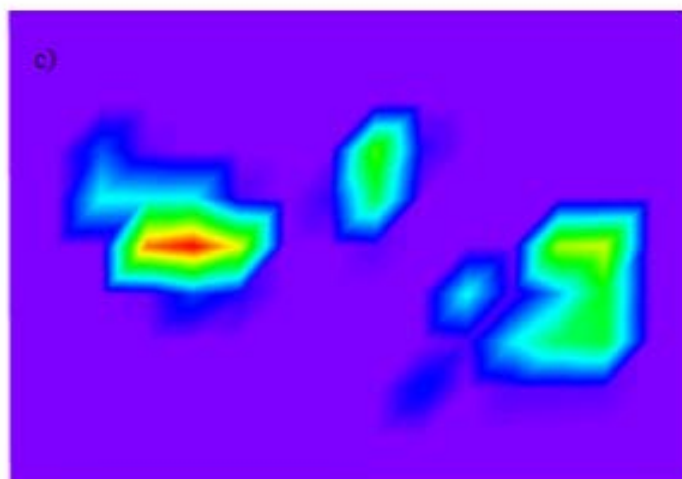
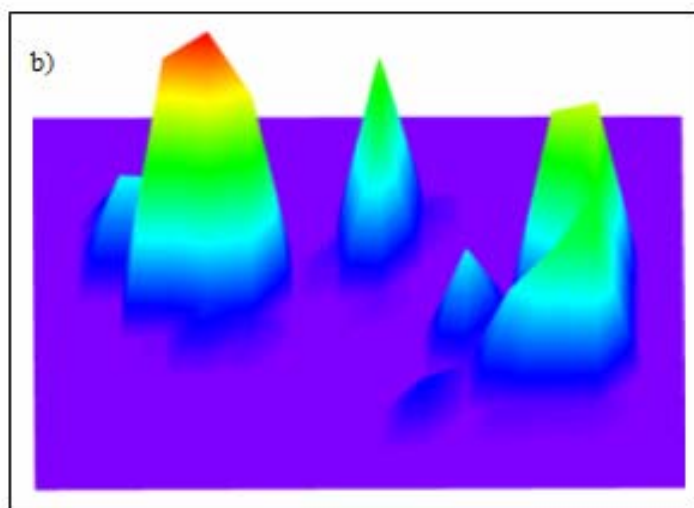
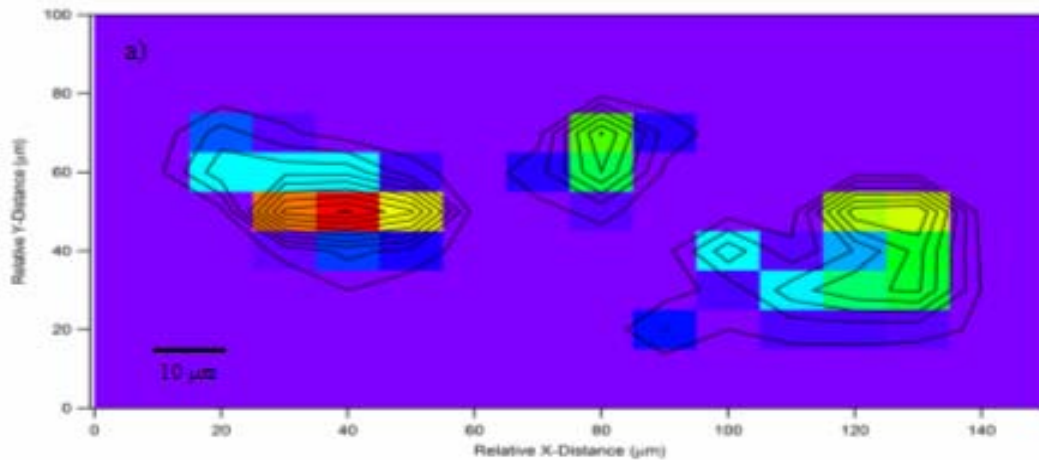


Figure 4.6: a) Contour plot of d_{62} -DPPC vesicles on the surface of a coverslip, b) 3-D plot of the CH_2 -SS intensity distribution of the d_{62} -DPPC vesicles on a coverslip, and c) False color image of d_{62} -DPPC vesicles based on the presence of the CH_2 -SS.

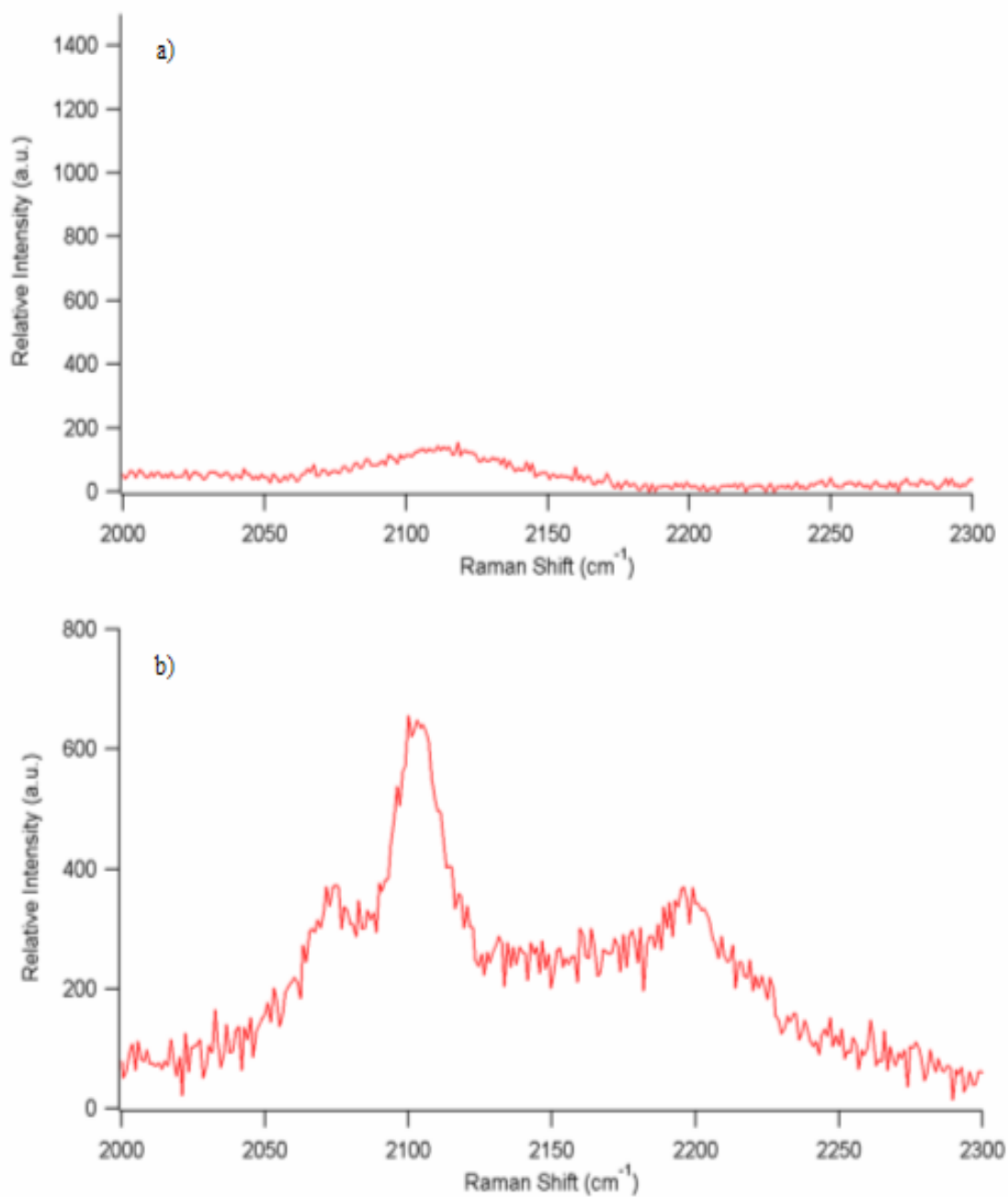


Figure 4.7: Spectra of a coverslip containing d62-DPPC vesicles in a) a region showing no Raman band intensity, and b) a region of high Raman band Intensity.

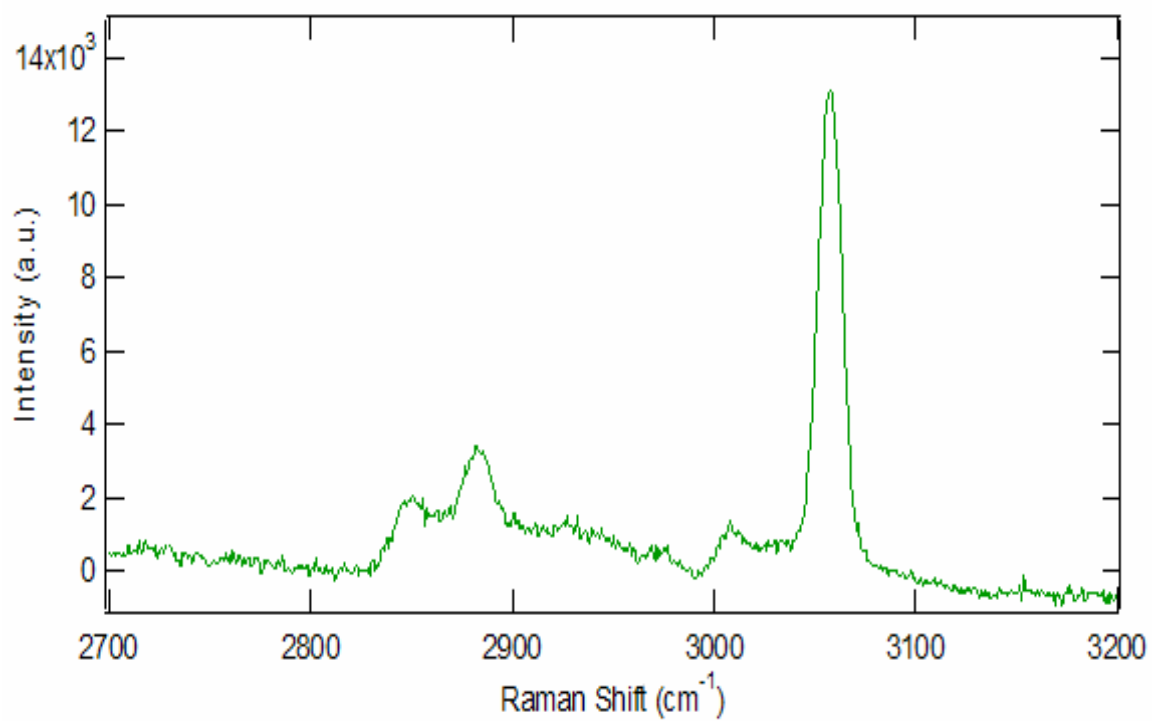


Figure 4.8: Raman spectrum of the bulk microscope coverslip covered with microscopic crystals of naphthalene and palmitic acid.

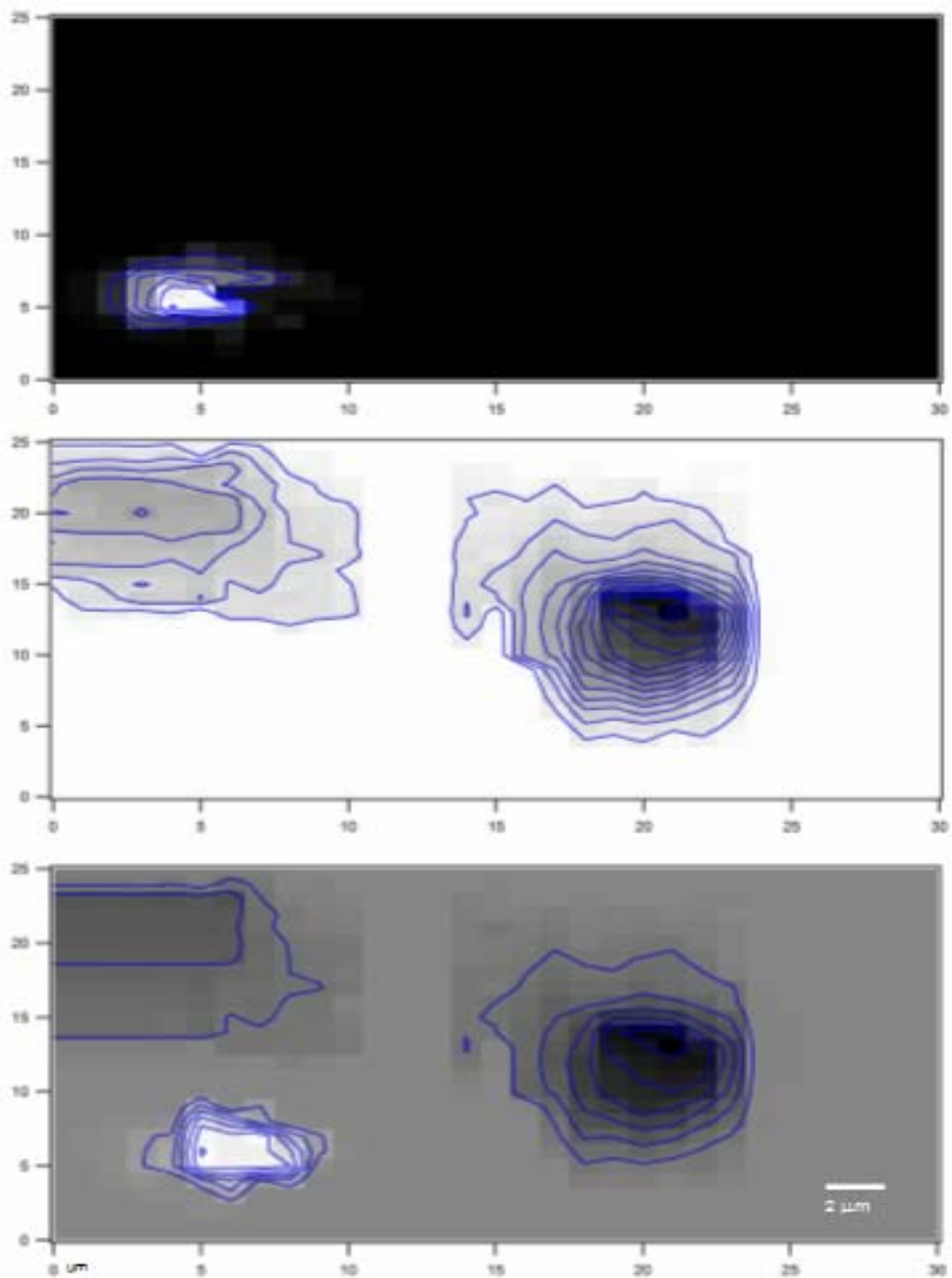


Figure 4.9: Contour plots of a microscope coverslip imaged base on a) the C-H stretch of naphthalene (3056 cm^{-1}), b) the $\text{CH}_2\text{-AS}$ of palmitic Acid (2880 cm^{-1}), and c) the combined Contour plot showing naphthalene in white and palmitic acid in black.

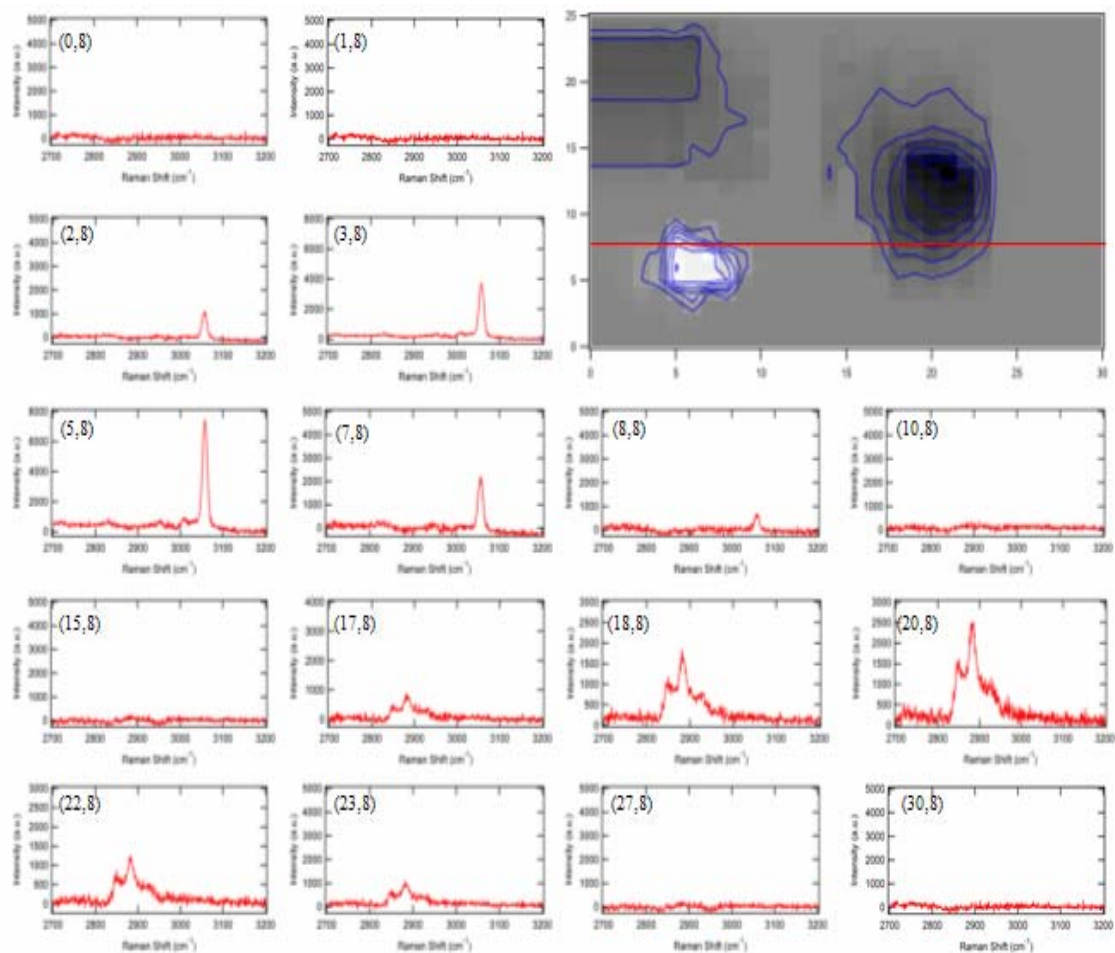


Figure 4.10: Selected spectra taken along the red ($Y=8$) line of the contour plot of naphthalene and palmitic Acid. The position of each spectrum is noted in the upper left corner of the spectrum. The peak at 3056 cm^{-1} indicates the presence of naphthalene and the peak at 2880 cm^{-1} indicates the presence of palmitic acid.

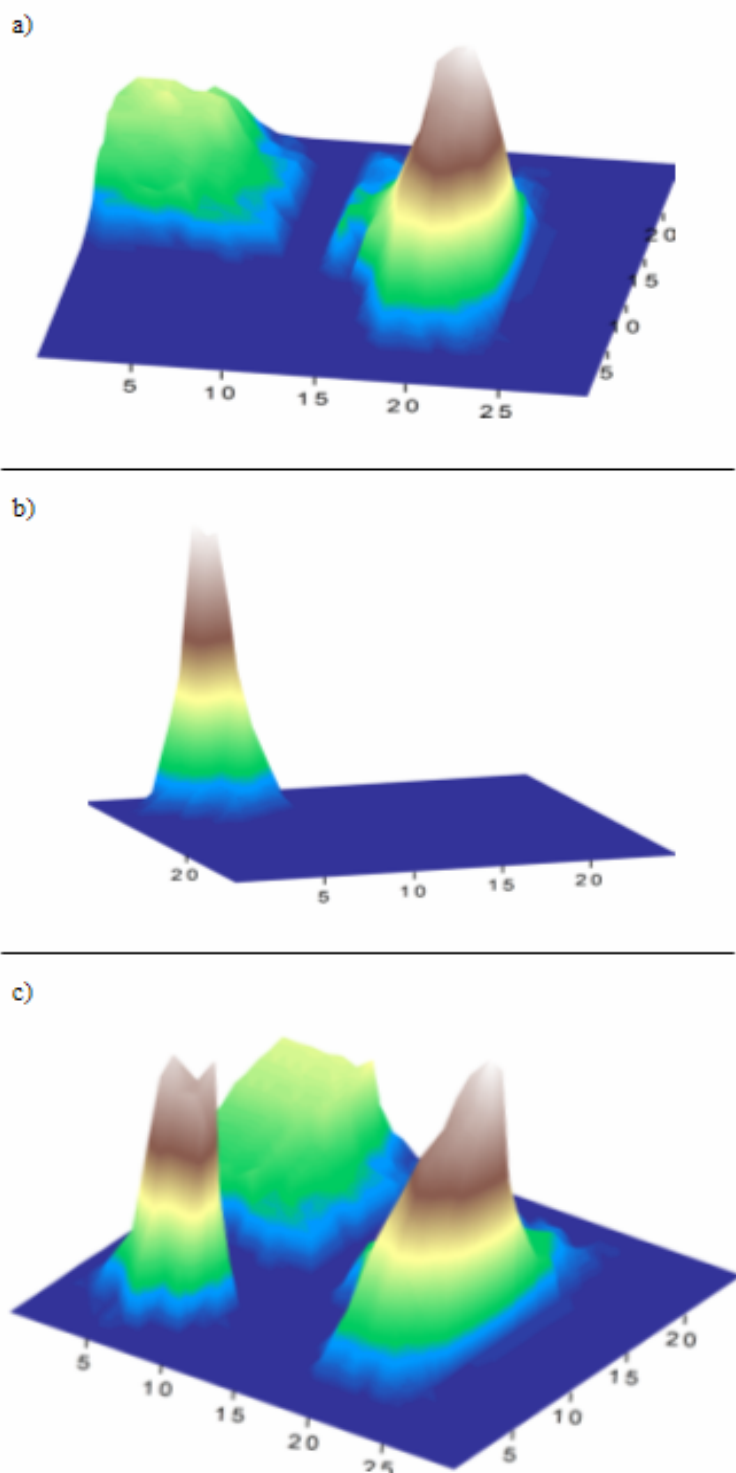


Figure 4.11: Three-Dimensional intensity distribution of naphthalene and palmitic acid crystals on microscope coverslip based on a) $\text{CH}_2\text{-AS}$ of palmitic acid, b) C-H stretch of naphthalene, and c) the combined intensity distribution of both types of crystals.

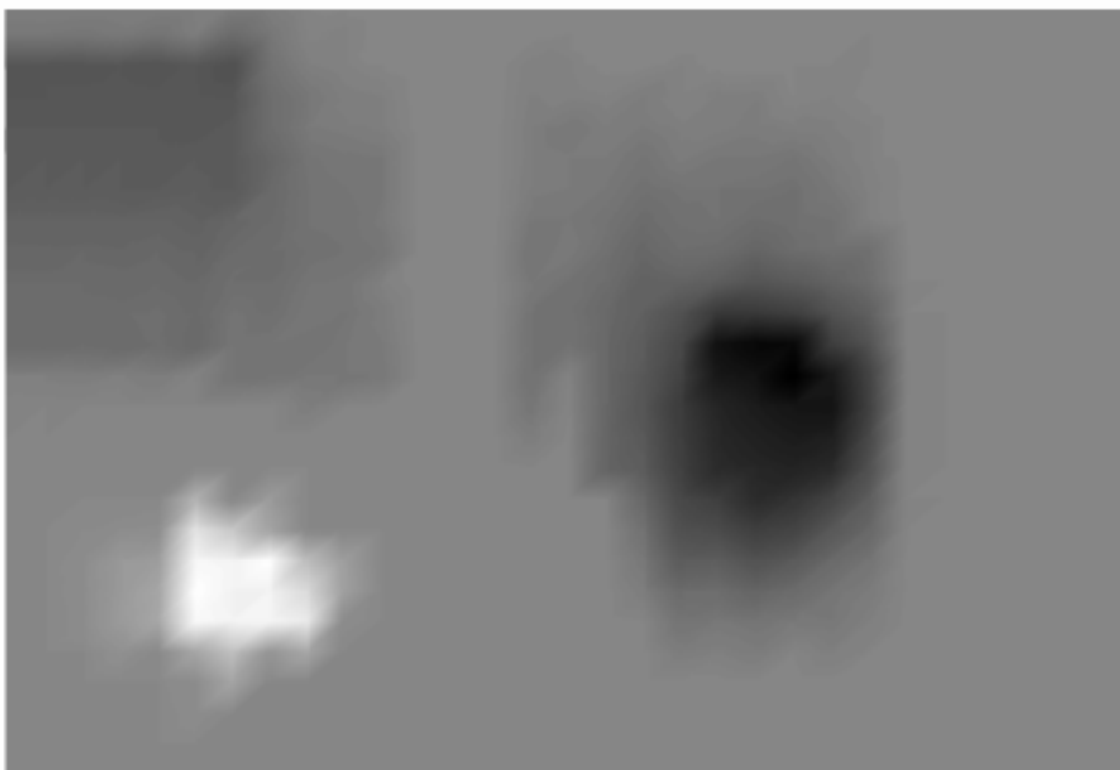


Figure 4.12: *Microspectroscopic false color image of a microscope coverslip based on the C-H stretch of naphthalene (in white) and the CH₂AS of palmitic acid (in black). Zero spectral intensity is represented by the color gray.*

LIST OF REFERENCES

- (1) Laserna, J. J. *Modern Techniques in Raman Spectroscopy*; Wiley: Chichester; New York, 1996.
- (2) Muggli, Z.; Anderson, M. E. *Solid State Technology* **1985**, 28, 287-291.
- (3) Toribara, T. Y.; University of Rochester. Dept. of Radiation, Biology and Biophysics. *Environmental Pollutants: Detection and Measurement*; Plenum Press: New York, 1978.
- (4) Finlayson-Pitts, B. J.; Pitts, J. N. *Chemistry of the Upper and Lower Atmosphere: Theory, Experiments and Applications*; Academic Press: San Diego, Calif., 2000.
- (5) Radhakrishnan, R.; Oyama, S. T.; Chen, J. G.; Asakura, K. *Journal of Physical Chemistry B* **2001**, 105, 4245-4253.
- (6) Li, W.; Oyama, S. T. *Journal of the American Chemical Society* **1998**, 120, 9047-9052.
- (7) Merlin, J. C.; Turrell, S.; Huvenne, J. P. *Spectroscopy of Biological Molecules*; Kluwer Academic Publishers: Dordrecht; Boston, 1995.
- (8) Nabiev, I.; Chourpa, I.; Manfait, M. *Journal of Raman Spectroscopy* **1994**, 25, 13-23.
- (9) Morris, M. D.; Finney, W. F.; Rajachar, R. M. *Faraday Discussions* **2004**, 126, 159-168.
- (10) McCreddie, B. R.; Morris, M. D.; Chen, T. C. *Journal of Bone and Mineral Research* **2003**, 18, S56-S57.
- (11) Bonera, E.; Fanciulli, M.; Batchelder, D. N. *Applied Physics Letters* **2002**, 81, 3377-3379.
- (12) Bonera, E.; Fanciulli, M.; Batchelder, D. N. *Journal of Applied Physics* **2003**, 94, 2729-2740.
- (13) Haka, A.; Shafer-Peltier, K. E.; Fitzmaurice, M.; Crowe, J.; Myles, J.; Dasari, R. R. *Cancer Research* **2002**, 62, 5375-5380.
- (14) McNaughton, D.; Wood, B. *Journal of Biomedical Optics* **2005**, 10.

- (15) Kozloff, K. M.; Carden, A.; Bergwitz, C. *Journal of Bone and Mineral Research* **2004**, *19*, 614-622.
- (16) Tarnowski, C. P.; Ignelzi, M. A.; Wang, W. *Journal of Bone and Mineral Research* **2004**, *19*, 64-71.
- (17) Chen, I.; Chu, S.; Bresson, F.; Tien, M.; Shi, J.; Sun, C. *Optics Letters* **2003**, *28*, 1338-1340.
- (18) Levin, I. W.; Bhargava, R. *Annual Review of Physical Chemistry* **2005**, *56*, 429-474.
- (19) Habuchi, S.; Cotlet, M.; Gronheid, R.; Dirix, G.; Michiels, J.; Vanderleyden, J.; De Schryver, F. C.; Hofkens, J. *Journal of the American Chemical Society* **2003**, *125*, 8446-8447.
- (20) Cheng, J.; Xie, X. S. *Journal of Physical Chemistry B* **2004**, *108*, 827-840.
- (21) Potma, E. O.; Xie, X. S. *Journal of Raman Spectroscopy* **2003**, *34*, 642-650.
- (22) Nan, X. L.; Cheng, J.; Xie, X. S. *Journal of Lipid Research* **2003**, *44*, 2202-2208.
- (23) Skoog, D. A.; Leary, J. J. *Principles of Instrumental Analysis*, 4 ed.; Saunders College Publishing: Philadelphia, 1992.
- (24) Long, D. A. *The Raman Effect: A Unified Treatment of the Theory of Raman Scattering by Molecules*; John Wiley & Sons: New York, 2001.
- (25) Dettman, J. W. *Introduction to Linear Algebra and Differential Equations*; McGraw-Hill Book Company: New York, 1986.
- (26) Ingle, J. D.; Crouch, S. R. *Spectrochemical Analysis*; Prentice Hall: New York, 1988.
- (27) McCreery, R. L. *Raman Spectroscopy for Chemical Analysis*; John Wiley & Sons: New York, 2000.
- (28) Turrell, G.; Corset, J. *Raman Microscopy: Developments and Applications*; Harcourt Brace: London; San Diego, 1996.
- (29) DelhayeDelhaye, M.; Dhamelincourt, P. *Journal of Raman Spectroscopy* **1975**, *3*, 33.
- (30) Bowden, M.; Gardiner, D. J.; Rice, G.; Gerrard, D. L. *Journal of Raman Spectroscopy* **1990**, *21*, 37-41.

- (31) Delhaye, M.; Bridoux, M.; Wallart, F. *Journal of Molecular Structure* **1982**, 79, 51-66.
- (32) Hirschfeld, T. *Journal of the Optical Society of America* **1973**, 63, 476.
- (33) Hudson, B. S. *Annual Review of Biophysics and Biophysical Chemistry* **1977**, 6, 257.
- (34) Maker, P. D.; Terhune, R. W. *Physical Review* **1965**, 137, A801-818.
- (35) Begley, R. F.; Harvey, A. B.; Byer, R. L. *Applied Physics Letters* **1974**, 25, 387-390.
- (36) Zumbusch, A.; Holtom, G. R.; Xie, X. S. *Physical Review Letters* **1999**, 82, 4142-4145.
- (37) Zumbusch, A.; Holtom, G. R.; Xie, X. S. *Physical Review Letters* **1999**, 82, 4014.
- (38) Wilson, T. *Confocal Microscopy*; Academic Press: London, 1990.
- (39) Cheng, J.; Volkmer, A.; Xie, X. S. *Journal of the Optical Society of America B-Optical Physics* **2002**, 19, 1363-1375.
- (40) ASTM. *ASTM Designation E* **1998**, 1840-1896.
- (41) Ma, G.; Allen, H. C. *Langmuir* **2006**, 22, 5341-5349.
- (42) Lipp, M. M.; Lee, K. Y. C.; Waring, A.; Zasadzinski, J. A. *Biophysical Journal* **1997**, 72, 2783-2804.
- (43) Bringezu, F.; Ding, J.; Brezesinski, G.; Zasadzinski, J. A. *Langmuir* **2001**, 17, 4641-4648.
- (44) Hill, I. R.; Levin, I. W. *Journal of Chemical Physics* **1979**, 70, 15.

APPENDIX A

RAMAN MICROSCOPE STAGE COORDINATION USING LABVIEW 7.1

The aim of this research is to recreate the image of a sample from its unique molecular vibrational spectrum. To accomplish this task, a routine was created to coordinate the X and Y position of the sample stage to the spectrum that was obtained at that position. An interface was developed to allow communication between a digital readout displaying the relative position of the microscope stage and the computer connected to the spectrometer acquiring spectral data. This type of interface was not commercially available with the purchase of the digital readout so a communication interface was programmed in LabView 7.1. The following appendix will detail the LabVIEW interface, how to use it, and how to interpret the acquired data. A working knowledge of LabVIEW programming language will be helpful but not necessary to follow this procedure.

A.1: LabVIEW Serial Port Communication Interface Modification

The microscope stage is connected to a Boeckeler Instruments Microcode II digital readout device by two linearly encoded cables. The purpose of the digital readout is to translate the motion of the stage into the distance moved in micrometers (μm). The displayed value can either be an absolute distance from the true zero position of the microscope stage, or as a relative distance from a user defined zero position. For

convention, the distances used are all relative distances from the user defined zero. The user defined zero is the position where the data acquisition of a sample is to begin. The Boeckeler Instruments Microcode II digital readout is equipped with an RS-232 serial port to output a data string which can be read by a computer.

The Raman Microscope Coordinate Control interface is a modification of the Basic Serial Read/Write interface available in LabView. By changing the user defined variables to those in Table A-1, the interface was able to communicate with the digital readout device connected to the microscope and to display the exact coordinates of the microscope stage. The user defined variables that needed to be modified to allow the example code to be able to properly recognize the data being output by the digital readout were VISA resource name, baud rate, data bits, parity, stop bits, and the flow control. The VISA resource name refers simply to which serial port of the computer the RS-232 cable is plugged into. In this case the VISA resource name was set to COM1, signifying that the RS-232 cable was plugged into COM port, or serial port, one. The baud rate is a measure of how fast data is moving between instruments using serial communication. It is the number of times per second a signal in a communications channel changes state. A baud rate of 600 was chosen to match the output rate of the digital readout. The data bits variable was defined as eight because the data being sent by the digital readout to the computer was binary. The parity variable was set to zero because we are not concerned with whether the data transmitted is true or false. We are only concerned with reading the values sent by the digital readout. The stop bits variable defines how many bits of information the computer should expect to signal the end of a data string. The stop bits variable was set at one bit to match the output of the digital readout device. The flow

control of a device is needed when the transmitted data is being sent or received at a variable speed. Because the data transmitted from the digital readout is sent at a constant speed the flow control was set to none.

Once all of the user defined variables were correct, the Basic Serial Read/Write interface was able to properly communicate and display the same value as was displayed on the digital readout. To save the position (or XY data), a “*Write Characters to File*” program was imbedded into the timed loop of the basic interface. The “*Write Characters to File*” program reads the values that are displayed in the read portion of the interface and then writes them to a user defined text file. The text file is created before data acquisition commences and the path to this file must be specified in the block diagram of the program for the interface to function properly. Figure A-1 shows an example of the block diagram for the *Raman Microscope Coordinate Control Interface*.

A.2: Operation of the Raman Microscope Coordinate Control Interface

The purpose for writing a program to communicate between the digital readout and the computer is to record the position of the stage during the acquisition of a Raman spectrum. This information is then used at a later time to create an image of a sample. This section will provide an overview of the steps that should be followed when running the *Raman Microscope Coordinate Control* interface so as to allow for proper recording of the stage position during data acquisition.

- 1) Turn on Boeckeler Instruments Microcode II digital readout before opening the interface. If the digital readout is turned on after the interface is opened up the interface will not be able to communicate with the digital readout.

- 2) Open Raman Microscope Coordinate Control by double clicking the desktop icon.
- 3) Select “Window” from the navigation bar at the top of the program. Select the option “Tile up and down”. This will bring up both the front panel and the block diagram of the interface.
- 4) Create a text document to save position data to by right clicking the mouse on the desktop and selecting “New” and then selecting “text document”. Give this text document a unique name.
- 5) In the block diagram change the path of the “*Write Characters to File*” program by right clicking on the path dialog box of the program and selecting the “browse for path...” option.
- 6) Browse for the text file recently created and click save in the dialog box. The interface will now store the position data in this file.
- 7) Close the block diagram screen of the interface and locate the front panel of the interface, see figure A-2. The front panel will be where you control the position data acquisition.
- 8) To run the program simply click on the “run” arrow located navigation bar at the top of the screen. The grid lines of the front panel will disappear signifying that the interface is running. The window “Microcode II X & Y Position” will display the coordinates displayed on the digital readout.
- 9) After recording the spectral data at the first microscope stage position click on the “**Take Position Data**” button on the front panel. This will read the microscope stage position and save it to the text file that was created. Be

careful to only press the button once per spectral data point, because every time the button is pressed a position data set is recorded to the test file.

- 10) After a spectrum at a particular point is acquired, move the microscope stage to its next position using the micrometer arm connected to the stage.
- 11) Continue with steps 9 and 10 until all points of the raster scan have been completed.
- 12) Once image acquisition is complete press “**Stop**” on the front panel to stop the interface and ensure that no extraneous position points are added to the text file.
- 13) Close the *Raman Microscope Coordinate Control interface*.

If all of these steps have been followed correctly, the number of positional data points in the text file will equal the number of Raman spectra acquired.

A.3: Preparation of Microscope Position Data for use in Image Generation.

The result of properly using the Raman Microscope Coordinate Control interface will be a text file containing a record of every microscope position where a Raman spectrum was acquired. The data in the text file is in the form X+0.0000Y+0.0000 for the coordinate position (0.0000, 0.0000). Although the text file is tab delimited the form of the data is not such that Igor Pro can distinguish between the X and Y positions of the data. The data must first be reformatted before loading it into Igor Pro, the image generation used. To reformat the X and Y position data:

- 1) Open a blank Microsoft Excel workbook.

- 2) From the navigation bar in Excel select “Open” and then browse for the text file created to store the position data. Once the text file is located choose “Open”.
- 3) Excel will offer two options when opening a text file either “Delimited” or “Fixed Width”. Select “Fixed Width” radio button. Fixed width allows the user to define where the columns of data begin and end.
- 4) Click on the “Next” button.
- 5) To create column breaks left click the mouse where the column breaks are. Set the breaks at these points: X | +0.0000 | Y | +0.0000 (the vertical lines represent the column breaks).
- 6) After the column breaks have been properly set press “Next”.
- 7) For the columns containing the markers X and Y select the radio button labeled “Do Not Import Column (skip)” which will exclude these columns from the spreadsheet. For the numerical position columns select the radio button labeled “General” which will load these values as general numeric values into the spreadsheet.
- 8) Press “Finish” to complete the creation of the position spreadsheet.

Save the spreadsheet with a unique name. This file will be imported into Igor Pro. This spreadsheet is the “Microscope Position Spreadsheet” to be loaded into Igor as outlined in Appendix B.

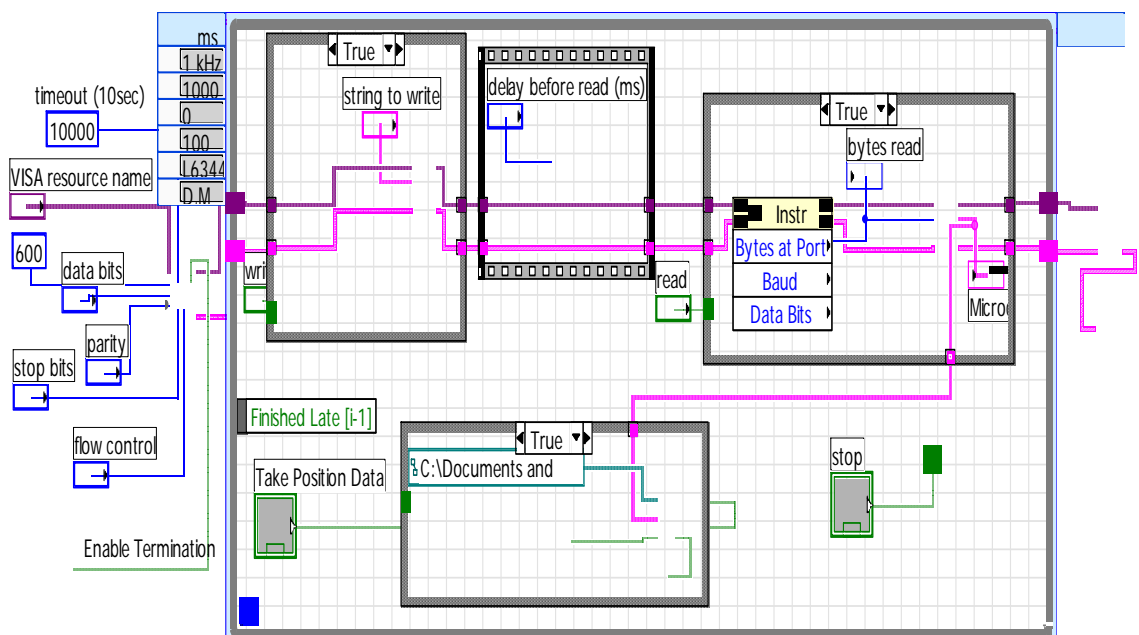


Figure A.1: Raman Microscope Coordinate Control LabVIEW Block Diagram.

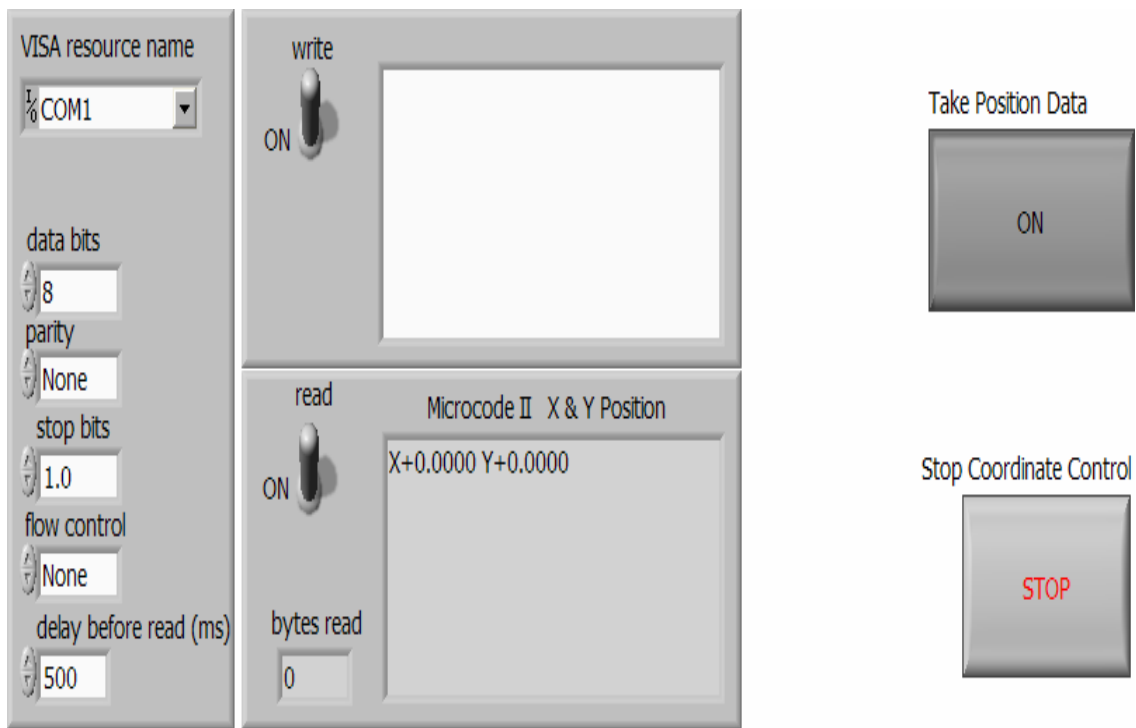


Figure A.2: Raman Microscope Coordinate Control LabVIEW Front Panel.

Variable Name	Default Setting	Raman Microscope Setting
Visa Resource Name	None	COM1
Baud Rate	2600	600
Data Bits	6	8
Parity	Even	0
Stop Bits	0	1
Flow Control	Variable	None

Table A.1: *User defined variables for Raman Microscope Coordinate control in LabVIEW.*

APPENDIX B

RAMAN MICROSPECTROSCOPIC IMAGE GENERATION USING IGOR PRO 4.

Images of a sample are obtained through Raman microspectroscopic imaging by acquiring spectral data of a sample in a point by point basis while raster scanning the stage of the microscope. The result of imaging a sample in this fashion is the accumulation of hundreds of spectra for each sample. The exact number of spectra obtained is dependent on the size of the sample and the step size of the image. Contour plots, surface plots, and false color image plots are all created by plotting peak intensity versus the X and Y coordinates. The peak intensity is defined as the integrated area under a desired spectral peak. Igor Pro 4.0 by WaveMetrics was used to quickly and efficiently process vast amounts of data as well as to generate clear images of the processed data. A macro was written in Igor Pro to perform these tasks.

B.1: Procedure – Using Igor Pro for Raman Microspectroscopic Data

This section describes the routine used to process the spectroscopic data obtained from the Raman Microscope to create an image. An example of the written routine in Igor Pro is provided at the end of this section.

- 1) Open procedure file in Igor Pro to start data analysis.
 - a) Click on “File”
 - b) Select “Open File”

- i) Select "Procedure..."
 - ii) Browse for "Raman Microscope.ipf"
 - iii) Select "Raman Microscope.ipf"
 - iv) Click "Open"
- 2) Edit procedure file to suite your data and acquisition parameters.
- a) Change # in the command line of the macro, limB= #, to the number of background spectra taken for the sample.
 - b) Change # in the command line of the macro, limM= #, to the number of spectra taken of the sample.
 - c) Change # in the command line of the macro, make/o/d/n= # peakarea, to the number of spectra taken of the sample
 - d) Specify the file location where your data is stored in the command line macro, NewPath/O path "___". This will be the colon delimited path to the folder storing background and sample data files. For example:
NewPath/O path "C:Documents and Settings:Desktop:Palmitic Acid:Image:"
 - e) Specify the common background file name in the command line of the macro, bkgdfile="___". This will be the base file name of all of the background spectra taken. For example: *bkgdfile="Background_"*
 - f) Specify the common file name for your spectral data in the command line of the macro, basefile="___". This will be the basefile name of all the spectral data taken of the sample. For example: *basefile="PA-Naph_"*

- g) Specify the file location of the microscope position data Excel spreadsheet in the command line, `XLLoadWave/S="___"`. This will be the colon delimited path to the Excel spreadsheet containing the X and Y positions of the microscope stage during spectral acquisition. For example:

```
XLLoadWave/S="Microscope Position Data"/R=(A1,B546)/D/A=wave  
"C:Documents and Settings:Palmitic Acid:Image:Microscope Position  
Data.xls"
```

- i) The creation of the microscope position data spreadsheet is outlined in Appendix A of this thesis.
- h) Change p1 and p2 in the command line, `peakarea1[n]=area($wave1name, p1, p2)`, to points at the base of the spectral peak being analyzed.
- i) Do this for each subsequent peak of interest in the spectrum.
- i) Click “Compile” at the bottom of the procedure window to exit the macro.
- 3) Run the Raman Microscope procedure.
- a) Type `raman()` into the command line of the command window, not the macro window.
- b) Press “Enter” to execute the procedure.

When all of the user defined variables have been properly edited and the macro is run the following results will be obtained:

- 1) The background spectra are averaged and displayed in a graph.
- 2) The sample spectra have the average background subtracted from them and are loaded as waves.

- 3) The background subtracted waves are each individually loaded and displayed in a table along with the Raman Shift x-axis.
- 4) The X and Y positions of the microscope stage are individually loaded as waves.
- 5) The peak areas of the spectral peak of interest are calculated and loaded as waves.
- 6) A table of X position, Y position, and peak area is created and displayed.

This data is used to generate the category plots, contour plots, surface plots and false color image plots that are shown in this thesis. Section B.2 will outline how these plots are created.

The routine written to analyze the data as described in the above section is shown below:

```
#pragma rtGlobals=1           // Use modern global access method.
#include <Waves Average>

Macro raman()
  Silent 1

  KillWaves/A/Z

  string filename, wave0name, wave1name, normname, bkgdfile, basefile,
  bkgdavename, xaxisname
  string numstring

  variable/g m, b, limM, limB,d, GaAs_max, x1,x2, n

  b = 0
  limB= #                       //number of background spectra
  m = 0
  limM = #                       //number of sample spectra
  n=0

  make/o/d/n= # peakarea1       //change number to # of spectra to be analyzed
```

```

make/o/d/n= # peakarea2
make/o/d/n= # peakarea3

NewPath/O path "___" //specify file location of data
bkgdfile="___" //specify the common background data file name
basefile="___" //specify the common spectral data file name

XLLoadWave/S="Microscope Position Data"/R=(A1,B260)/D/A=wave "___"
//specify microscope position data spreadsheet

rename wave0, xposition
rename wave1, yposition

do

filename = bkgdfile + num2str(b) + ".asc"
LoadWave/G/A/P=path filename

if (b==0) then

    wave0=1e7*(1/785-1/wave0)
    xaxisname=basefile + "_xaxis"
    rename wave0, $xaxisname

else

    KillWaves wave0

Endif

wave1name = bkgdfile + "_" + num2str(b)
Rename wave1, $wave1name

if (b == 0) then

    Display $wave1name vs $xaxisname as bkgdfile + " data"
Else

    AppendtoGraph $wave1name vs $xaxisname

endif

ModifyGraph tick=2,mirror=1
Label left "Intensity (a.u.)"
Label bottom "Raman Shift (cm\\S-1\\M)"

```

```

if (b==0) then

    duplicate $wave1name, bkgdadd
    bkgdadd=$wave1name
    duplicate bkgdadd, bkgdave

else

    bkgdadd=(bkgdaddave1name)

endif

    bkgdave=bkgdadd/(b) //computes average background
    b=b+1

while (b<limB)

    Append bkgdave vs $xaxisname
    ModifyGraph rgb(bkgdave)=(0,0,0)

do

    sprintf numstring, "%05d", (m)
    filename = basefile + numstring + ".asc"

    LoadWave/G/A/P=path filename
    KillWaves wave0

    wave1=(wave1-bkgdave)
    wave1name = basefile + "_" + numstring + ".au"

    Rename wave1, $wave1name

    if (m == 0) then

        Edit $xaxisname,$wave1name

    else

        AppendToTable $wave1name

    endif

    peakarea1[n]=area($wave1name, p1, p2)
    //calculates peak area between point's p1 & p2
    peakarea2[n]=area($wave1name, p1, p2)

```

```

peakarea3[n]=area($wave1name, p1, p2)

m = m + 1
n= n+1

while (m<limM)
    bkgdavename=bkgdfile+ "bkgdave"

    rename bkgdave, $bkgdavename
    edit xposition, yposition, peakarea1, peakarea2, peakarea3

end

```

B.2: Image Creation using Igor Pro

Igor Pro by WaveMetrics allows for the generation of many different types of plots or graphs to be created with the proper data sets. Creating category, contour, surface or image plots in Igor is done using either X, Y, Z waves, or a matrix of Z values. Using a matrix of Z values to create these plots provides cleaner, clearer looking plots and thus should always be used when creating plots. The proper creation of these plots is necessary to accurately portray a sample image. This section explains the creation of a matrix of Z values, as well as the creation of category, contour, surface and image plots in Igor when using a matrix of Z values.

B.2.1: Creating a Matrix of Z Values for use in Igor Pro.

The creation of a matrix of Z values is imperative when creating images of the highest quality in Igor. A matrix of Z values is a spreadsheet of X and Y stage positions and the spectral data values of Z coordinated together. A spreadsheet is created in the form of the X positions of the spectral data in column A and the Y positions of the spectral data in row 1. A matrix is then created when the spectral data points, peak areas or intensities in this case, are coordinated into the proper position of the spreadsheet. The

proper configuration of the matrix should resemble Figure B-1 where the placement of a Z data point is coordinated with its X and Y positions.

The most efficient way to create this matrix of Z values is to open the Microsoft Excel workbook that was created to store the X and Y stage position data and create a matrix of Z values in the subsequent sheets of this workbook. The following steps should be taken to create a matrix of Z values.

- 1) Open Microscope Position Data Excel workbook.
 - a) Insert a row before row 1 and label Column A, X, and Column B, Y.
 - b) Copy and paste peak areas from Igor into the columns following the X and Y data already present.
 - c) Highlight all of the columns that contain data and then select “Data” from the toolbar. Selecting the data from the top of the columns will ensure that all of the rows will stay intact during the sorting of the data. This will order your data so that all of the data with similar Y-positions are grouped and then ordered by the X-position. This will ease in the transfer of data from this spreadsheet to the matrix format.
 - i) Select “Sort”
 - ii) Select “Sort by Y”
 - iii) Select “Then by X”
 - d) Select a new sheet in the Excel workbook.
 - i) Starting in Row 2 of Column A type the first X position.
 - ii) Continue typing the X positions in Column until all of the X positions have been entered into this new format.

- iii) Starting in Column 2 of Row 1 type the first Y position.
- iv) Continue typing the Y positions in Row1 and progressing across the columns until all of the Y positions have been entered into this format.
- e) Go back to the spreadsheet containing the X, Y, and peak area data.
 - i) Highlight all of the peak areas that correspond to a given Y position.
 - ii) Right click the mouse and select “Cut”.
 - iii) Go to the Matrix spreadsheet.
 - iv) Select the first cell corresponding to the desired Y position of the matrix.
 - v) Right click the mouse and select “Paste”.
 - vi) Continue this until the entire given peak area data is in this matrix format.
- f) Select “File”.
 - i) Select “Save as...”
 - ii) Select “Text (Tab delimited)” and give the matrix a unique name.
 - iii) Select “Save”.

The matrix of Z values is now created and saved in a format that is recognizable by Igor Pro. This procedure should be followed for every peak area that is to be imaged.

B.2.2: Creating Contour, Image and Surface plots in Igor Pro.

An advantage of a spectroscopic imaging system is the ability to arrive at graphical representations of a sample based on a molecular signature which accurately

portrays the sample. With the proper use of the image software these graphical representations of a sample can be made to be both aesthetically pleasing to the eye and informative. The following section details how to create contour plots, image plots, and surface plots using data that has been.

Contour Plots. Igor defines a contour plot as a two-dimensional XY plot of a three-dimensional XYZ surface showing lines where the surface intersects planes of constant elevation (Z). The contour plot is appropriate when data sets of the form, $Z = f(x, y)$, are used (meaning there is only one Z value for each XY pair). A contour map is appropriate when depicting the Raman intensity distribution of a sample. To create a contour map in Igor:

- 1) Load spectral data matrix as a wave in Igor.
 - a) Select “Data”.
 - b) Select “Load Waves”.
 - i) Check the box indicating “Load Columns into Matrix”.
 - ii) Browse for the matrix of Z values file created from the X and Y positions and spectral data.
 - c) Click “Do it”.
- 2) Create the contour plot.
 - a) Click on “Windows”.
 - i) Select “New”.
 - ii) Select “Contour Plot”.
 - b) Under the Contour Data pull down menu select “Matrix of Z Values”.
 - i) Select the wave name loaded previously.

- ii) Change the appearance to fit desired settings
- iii) Click “Do It”.

Image Plots. Igor can display matrix data as an image plot in a graph window. Each matrix data value defines a colored rectangle in the image plot. The size and position of these rectangles is controlled by the range of the graph axes, the graph width and height modes, and the X and Y coordinates of the image rectangles. The images created in this mode are not true images, but false color images. False color images mean that the color gradient of the image is indicative of a change in scale, not a representation of the actual color of the object being imaged. Image plots are best at depicting a sample when the image plot is overlaid by a contour plot to outline the changes in intensity. The image plot is thus used to add further contrast to a contour plot. To create an image plot in Igor:

- 1) Load spectral data matrix as a wave in Igor.
 - a) If a contour plot or surface plot has already been created using a matrix of Z values then the data is already correctly loaded.
 - b) If a matrix of Z values has not been loaded already, follow the steps in section B.2.1.
- 2) Create an image plot.
 - a) Click on “Windows”.
 - i) Select “New”.
 - ii) Select “Image Plot”.
 - b) In the image plot dialog box select the desired wave name previously loaded as the source for the image plot.

- i) Change the appearance to the desired preferences of the image plot.
 - ii) Click “Do It”
- c) Append a contour plot to the newly created image plot.
- i) Click on “Graph”.
 - ii) Select “Append to Graph”.
 - iii) Select “Contour Plot”
 - iv) Select “Matrix of Z Values” from the contour plot dialog box
 - v) Select same wave name used to create image plot
 - vi) Click “Do It”

Surface Plots. Igor Surface Plotter is a data visualization tool that produces 3-dimensional surfaces, scatter plots and path plots from 2-D data. Surface plots are used as a visualization tool to represent the 3-dimensional intensity distribution of the Raman scattered light of a sample. Using the surface plotter to produce the 3-D intensity distribution recreates the distribution of the sample at the surface and provides insight into the amount of sample present. To create a surface plot in Igor using a matrix of Z values:

- 1) Load spectral data matrix as a wave in Igor.
 - a) If a contour plot or an image plot has already been created using a matrix of Z values then the data is already correctly loaded.
 - b) If a matrix of Z values has not been loaded already, follow the steps in the contour plot section.
- 2) Create a surface plot.

- a) Click on “Windows”.
 - i) Select “New”.
 - ii) Select “Surface Plot”.
- b) In the image plot dialog box select the desired wave name previously loaded as the source for the image plot.
 - i) Click “Do It”

There are several options that can be chosen to transform a surface plot into a more aesthetically pleasing representation of the data.

The first option is have the surface plotter provide a smoothed fit surface to the data:

- 1) Click on the “Controls” pull down menu of the open surface plot window.
- 2) Select the “Display Settings” option.
- 3) Click on the “Plot” pull down menu in the Display Settings window.
- 4) Select the “Smoother Fill” option.

The smoother fill option should be selected because in this mode each polygon is painted with a graduated fill based on the slope of the polygon. Other types of fill options can be chosen; however, this option yields the best fit of the data to a surface plot.

The second option that should be selected is to provide a “bottom image” for the surface plot. Adding a bottom image to a surface plot is equivalent to adding a contour plot to the bottom of the surface plot. This provides a frame of reference when viewing a surface plot to fully comprehend what is being depicted. To add a bottom image:

- 1) Under the “Display Settings” control menu select the Image Settings button.
- 2) Select the “Show Bottom Image” button.

- 3) Select “Use Main Source Wave”.
- 4) Select “Bilinear Interpolation”.
- 5) Press “Do It”.

This will result in a surface plot that shows a smooth fill of the data over a surface to yield a cleaner looking graph. The bottom image of the surface plot shows the image of the sample projected onto the microscope slide and should accurately correspond to the contour plots and image plots created from the same data set.

	Y_1	Y_2	Y_3	Y_4	Y_5
X_1	$Z_{1,1}$	$Z_{1,2}$	$Z_{1,3}$	$Z_{1,4}$	$Z_{1,5}$
X_2	$Z_{2,1}$	$Z_{2,2}$	$Z_{2,3}$	$Z_{2,4}$	$Z_{2,5}$
X_3	$Z_{3,1}$	$Z_{3,2}$	$Z_{3,3}$	$Z_{3,4}$	$Z_{3,5}$
X_4	$Z_{4,1}$	$Z_{4,2}$	$Z_{4,3}$	$Z_{4,4}$	$Z_{5,5}$
X_5	$Z_{5,1}$	$Z_{5,2}$	$Z_{5,3}$	$Z_{5,4}$	$Z_{5,5}$

Table B.1: *An example of a Z-Matrix used to aide in image reconstruction.*